A roadmap to control penguin effects in $B_d^0 \to J/\psi K_S^0$ and $B_s^0 \to J/\psi \phi$

Kristof De Bruyn[a] and **Robert Fleischer**[a,b]

[a] *Nikhef,*
Science Park 105, NL-1098 XG Amsterdam, Netherlands

[b] *Department of Physics and Astronomy, Vrije Universiteit Amsterdam,*
De Boelelaan 1081, NL-1081 HV Amsterdam, Netherlands

E-mail: debkr@nikhef.nl, Robert.Fleischer@nikhef.nl

Abstract: Measurements of CP violation in $B_d^0 \to J/\psi K_S^0$ and $B_s^0 \to J/\psi \phi$ decays play key roles in testing the quark-flavour sector of the Standard Model. The theoretical interpretation of the corresponding observables is limited by uncertainties from doubly Cabibbo-suppressed penguin topologies. With continuously increasing experimental precision, it is mandatory to get a handle on these contributions, which cannot be calculated reliably in QCD. In the case of the measurement of $\sin 2\beta$ from $B_d^0 \to J/\psi K_S^0$, the U-spin-related decay $B_s^0 \to J/\psi K_S^0$ offers a tool to control the penguin effects. As the required measurements are not yet available, we use data for decays with similar dynamics and the SU(3) flavour symmetry to constrain the size of the expected penguin corrections. We predict the CP asymmetries of $B_s^0 \to J/\psi K_S^0$ and present a scenario to fully exploit the physics potential of this decay, emphasising also the determination of hadronic parameters and their comparison with theory. In the case of the benchmark mode $B_s^0 \to J/\psi \phi$ used to determine the B_s^0-$\bar{B}_s^0$ mixing phase ϕ_s the penguin effects can be controlled through $B_d^0 \to J/\psi \rho^0$ and $B_s^0 \to J/\psi \bar{K}^{*0}$ decays. The LHCb collaboration has recently presented pioneering results on this topic. We analyse their implications and present a roadmap for controlling the penguin effects.

Contents

1 Introduction

The data of the first run of the Large Hadron Collider (LHC) at CERN have led to the exciting discovery of the Higgs boson [1, 2] and are, within the current level of precision, globally consistent with the picture of the Standard Model (SM). The next run of the LHC at almost the double centre-of-mass energy of the colliding protons, which will start in spring 2015, will open various new opportunities in the search for New Physics (NP) [3]. These will be both in the form of direct searches for new particles at the ATLAS and CMS experiments, and in the form of high-precision analyses of flavour physics observables at the LHCb experiment. Concerning the latter avenue, also the Belle II experiment at the KEK e^+e^- Super B Factory will enter the stage in the near future [4]. The current LHC data suggest that we have to prepare ourselves to deal with smallish NP effects, and it thus becomes mandatory to have a critical look at the theoretical assumptions underlying the experimental analyses.

Concerning measurements of CP violation, the $B_d^0 \to J/\psi K_S^0$ and $B_s^0 \to J/\psi \phi$ decays play outstanding roles as they allow determinations of the B_q^0-$\bar{B}_q^0$ mixing phases ϕ_d and ϕ_s, respectively. These quantities take the forms

$$\phi_d = 2\beta + \phi_d^{\mathrm{NP}}, \quad \phi_s = -2\lambda^2\eta + \phi_s^{\mathrm{NP}}, \tag{1.1}$$

where β is the usual angle of the unitarity triangle (UT) of the Cabibbo-Kobayashi-Maskawa (CKM) matrix [5, 6] and

$$\phi_s^{\mathrm{SM}} = -2\lambda^2\eta = -(2.086^{+0.080}_{-0.069})^\circ \tag{1.2}$$

in the SM [7]. The λ and η are two of the Wolfenstein parameters [8] of the CKM matrix. The CP-violating phases ϕ_q^{NP}, which vanish in the SM, allow for NP contributions entering through B_q^0-$\bar{B}_q^0$ mixing.

The theoretical precision for the extraction of ϕ_d and ϕ_s from the CP asymmetries of the $B_d^0 \to J/\psi K_S^0$ and $B_s^0 \to J/\psi \phi$ decays is limited by doubly Cabibbo-suppressed penguin contributions. The corresponding non-perturbative hadronic parameters cannot be calculated in a reliable way within QCD. However, in the era of high-precision measurements, these effects have to be controlled with the final goal to match the experimental and theoretical precisions [9–17].

As was pointed out in ref. [9], $B_s^0 \to J/\psi K_S^0$ is related to $B_d^0 \to J/\psi K_S^0$ through the U-spin symmetry of strong interactions, and allows a determination of the penguin corrections to the measurement of ϕ_d. Concerning the $B_s^0 \to J/\psi \phi$ channel, an analysis of CP violation is more involved as the final state consists of two vector mesons and thus is a mixture of different CP eigenstates which have to be disentangled through an angular analysis of their decay products [18, 19]. In this case, the decays $B_d^0 \to J/\psi \rho^0$ [10] and $B_s^0 \to J/\psi \bar{K}^{*0}$ [15] are tools to take the penguin effects into account. The LHCb collaboration has very recently presented the first polarisation-dependent measurements of ϕ_s from $B_s^0 \to J/\psi \phi$ in ref. [20]. We shall discuss the implications of these exciting new results in detail.

Since a measurement of CP violation in $B_s^0 \to J/\psi K_S^0$ is not yet available, we use the SU(3) flavour symmetry and plausible assumptions for various modes of similar decay dynamics to constrain the relevant penguin parameters. Following these lines, we assess their impact on the measurement of ϕ_d and predict the CP-violating observables of $B_s^0 \to J/\psi K_S^0$. In our benchmark scenario, we discuss also the determination of CP-conserving strong amplitudes, which will provide valuable insights into non-factorisable U-spin-breaking effects through the comparison with theoretical form-factor calculations.

Concerning the $B_s^0 \to J/\psi \bar{K}^{*0}$ channel, measurements of CP violation are also not yet available. However, in the case of $B_d^0 \to J/\psi \rho^0$, the LHCb collaboration has recently announced the first results of a pioneering study [21], presenting in particular a measurement of mixing-induced CP violation and constraints on the penguin effects. This new experimental development was made possible through the implementation of the method proposed by Zhang and Stone in ref. [22]. We shall have a detailed look at these exciting measurements and discuss important differences between the penguin probes $B_d^0 \to J/\psi \rho^0$ and $B_s^0 \to J/\psi \bar{K}^{*0}$. We extract hadronic parameters from the $B_d^0 \to J/\psi \rho^0$ data, allowing

insights into SU(3)-breaking and non-factorisable effects through a comparison with theory, and point out a new way to combine the information provided by the $B_s^0 \to J/\psi \bar{K}^{*0}$, $B_d^0 \to J/\psi \rho^0$ system in a global analysis of the $B_s^0 \to J/\psi \phi$ penguin parameters.

The outline of this paper is as follows: in section 2, we introduce the general formalism to deal with the penguin effects. In section 3, we explore the constraints of the currently available data for the penguin contributions to the $B_{d,s}^0 \to J/\psi K_{\rm S}^0$ system, while we turn to the discussion of the most recent LHCb results for $B_s^0 \to J/\psi \phi$ and the penguin probes $B_d^0 \to J/\psi \rho^0$, $B_s^0 \to J/\psi \bar{K}^{*0}$ in section 4. In section 5, we outline a roadmap for dealing with the hadronic penguin uncertainties in the determination of ϕ_d and ϕ_s. Finally, we summarise our conclusions in section 6.

2 CP violation and hadronic penguin shifts

For the neutral B_q decays ($q = d, s$) discussed in this paper, the transition amplitudes can be written in the following form [10]:

$$A(B_q^0 \to f) \equiv A_f = \quad \mathcal{N}_f \left[1 - b_f e^{\rho_f} e^{+i\gamma} \right] , \tag{2.1}$$

$$A(\bar{B}_q^0 \to f) \equiv \bar{A}_f = \eta_f \mathcal{N}_f \left[1 - b_f e^{\rho_f} e^{-i\gamma} \right] . \tag{2.2}$$

Here η_f is the CP eigenvalue of the final state f, $\mathcal{N}_f$ is a CP-conserving normalisation factor representing the dominant tree topology, b_f parametrises the relative contribution from the penguin topologies, ρ_f is the CP-conserving strong phase difference between the tree and penguin contributions, whereas their relative weak phase is given by the UT angle γ. The parameters $\mathcal{N}_f$ and b_f depend both on CKM factors and on hadronic matrix elements of four-quark operators entering the corresponding low-energy effective Hamiltonian.

In order to extract information on ϕ_q, CP-violating asymmetries are measured [23]:

$$\frac{|A(B_q^0(t) \to f)|^2 - |A(\bar{B}_q^0(t) \to f)|^2}{|A(B_q^0(t) \to f)|^2 - |A(\bar{B}_q^0(t) \to f)|^2} = \frac{\mathcal{A}_{\rm CP}^{\rm dir} \cos(\Delta M_q t) + \mathcal{A}_{\rm CP}^{\rm mix} \sin(\Delta M_q t)}{\cosh(\Delta \Gamma_q t/2) + \mathcal{A}_{\Delta\Gamma} \sinh(\Delta \Gamma_q t/2)} , \tag{2.3}$$

where the dependence on the decay time t enters through B_q^0-$\bar{B}_q^0$ oscillations, and $\Delta M_q \equiv M_{\rm H}^{(q)} - M_{\rm L}^{(q)}$ and $\Delta \Gamma_q \equiv \Gamma_{\rm L}^{(q)} - \Gamma_{\rm H}^{(q)}$ denote the mass and decay width differences of the two B_q mass eigenstates, respectively.

Using eqs. (2.1) and (2.2), the direct and mixing-induced CP asymmetries $\mathcal{A}_{\rm CP}^{\rm dir}$ and $\mathcal{A}_{\rm CP}^{\rm mix}$ take the following forms [10]:[1]

$$\mathcal{A}_{\rm CP}^{\rm dir}(B_q \to f) = \frac{2 b_f \sin \rho_f \sin \gamma}{1 - 2 b_f \cos \rho_f \cos \gamma + b_f^2} , \tag{2.4}$$

$$\mathcal{A}_{\rm CP}^{\rm mix}(B_q \to f) = \eta_f \left[\frac{\sin \phi_q - 2 b_f \cos \rho_f \sin(\phi_q + \gamma) + b_f^2 \sin(\phi_q + 2\gamma)}{1 - 2 b_f \cos \rho_f \cos \gamma + b_f^2} \right] , \tag{2.5}$$

---

[1]Whenever information from both $B_q^0 \to f$ and $\bar{B}_q^0 \to f$ decays is needed to determine an observable, as is the case for CP asymmetries or untagged branching ratios, we use the notation B_d and B_s.

while the observable $\mathcal{A}_{\Delta\Gamma}$ is given by

$$\mathcal{A}_{\Delta\Gamma}(B_q \to f) = -\eta_f \left[\frac{\cos\phi_q - 2b_f \cos\rho_f \cos(\phi_q + \gamma) + b_f^2 \cos(\phi_q + 2\gamma)}{1 - 2b_f \cos\rho_f \cos\gamma + b_f^2} \right] . \qquad (2.6)$$

For the discussion of the penguin effects, the following expression will be particularly useful (generalising the formulae given in ref. [15]):

$$\frac{\eta_f \mathcal{A}_{\mathrm{CP}}^{\mathrm{mix}}(B_q \to f)}{\sqrt{1 - \left(\mathcal{A}_{\mathrm{CP}}^{\mathrm{dir}}(B_q \to f) \right)^2}} = \sin(\phi_q + \Delta\phi_q^f) \equiv \sin(\phi_{q,f}^{\mathrm{eff}}) , \qquad (2.7)$$

where

$$\sin\Delta\phi_q^f = \frac{-2b_f \cos\rho_f \sin\gamma + b_f^2 \sin 2\gamma}{\left(1 - 2b_f \cos\rho_f \cos\gamma + b_f^2 \right) \sqrt{1 - \left(\mathcal{A}_{\mathrm{CP}}^{\mathrm{dir}}(B \to f) \right)^2}} , \qquad (2.8)$$

$$\cos\Delta\phi_q^f = \frac{1 - 2b_f \cos\rho_f \cos\gamma + b_f^2 \cos 2\gamma}{\left(1 - 2b_f \cos\rho_f \cos\gamma + b_f^2 \right) \sqrt{1 - \left(\mathcal{A}_{\mathrm{CP}}^{\mathrm{dir}}(B \to f) \right)^2}} , \qquad (2.9)$$

yielding

$$\tan\Delta\phi_q^f = -\left[\frac{2b_f \cos\rho_f \sin\gamma - b^2 \sin 2\gamma}{1 - 2b_f \cos\rho_f \cos\gamma + b_f^2 \cos 2\gamma} \right] . \qquad (2.10)$$

It should be emphasised that $\Delta\phi_q^f$ is a phase shift which depends on the non-perturbative parameters b_f and ρ_f and cannot be calculated reliably within QCD. In the case of $b_f = 0$, the following simple situation arises:

$$\mathcal{A}_{\mathrm{CP}}^{\mathrm{dir}}(B_q \to f)|_{b_f=0} = 0 , \qquad \eta_f \mathcal{A}_{\mathrm{CP}}^{\mathrm{mix}}(B_q \to f)|_{b_f=0} = \sin\phi_q , \qquad (2.11)$$

allowing us to determine ϕ_q directly from the mixing-induced CP asymmetry.

Since in the decays $B_d^0 \to J/\psi K_{\mathrm{S}}^0$ and $B_s^0 \to J/\psi\phi$ the parameters corresponding to b_f are doubly Cabibbo-suppressed, eq. (2.11) is approximately valid. However, in the era of high-precision studies of CP violation, we nonetheless have to control these effects. As the corresponding penguin parameters are Cabibbo-allowed in the $B_s^0 \to J/\psi K_{\mathrm{S}}^0$ and $B_d^0 \to J/\psi\rho^0$, $B_s^0 \to J/\psi\bar{K}^{*0}$ decays, these modes allow us to probe the penguin effects. Making use of the SU(3) flavour symmetry, we may subsequently convert the penguin parameters into their $B_d^0 \to J/\psi K_{\mathrm{S}}^0$ and $B_s^0 \to J/\psi\phi$ counterparts, where in the latter case also plausible dynamical assumptions beyond the SU(3) are required.

3 The $B_d^0 \to J/\psi K_{\mathrm{S}}^0$, $B_s^0 \to J/\psi K_{\mathrm{S}}^0$ system

3.1 Decay amplitudes and CP violation

In the SM, the decay $B_d^0 \to J/\psi K_{\mathrm{S}}^0$ into a CP eigenstate with eigenvalue $\eta_{J/\psi K_{\mathrm{S}}^0} = -1$ originates from a colour-suppressed tree contribution and penguin topologies with q-quark exchanges $(q = u, c, t)$, which are described by CP-conserving amplitudes C' and $P'^{(q)}$,
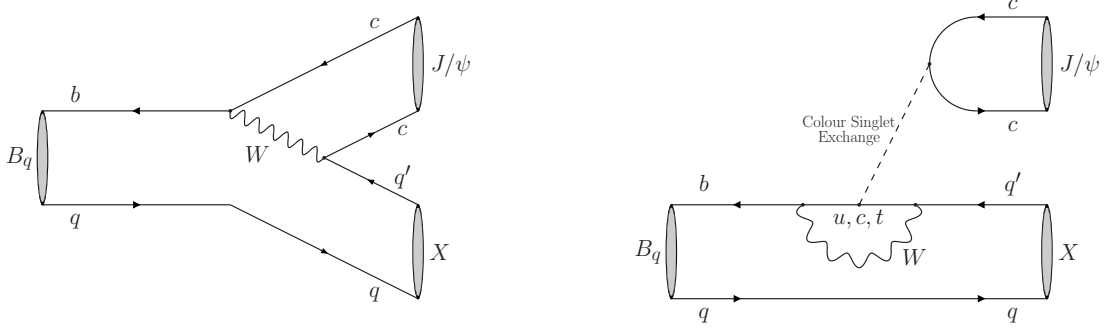
Figure 1. Illustration of tree (left) and penguin (right) topologies contributing to the $B_q \to J/\psi X$ channels, where $q \in \{u, d, s\}$, $q' \in \{d, s\}$ and X represents any of the π^0, π^+, K^+, K^0_S, ρ^0, ϕ^0 or $\overline{K}^{*0}$ mesons.

respectively, and illustrated in figure 1. The primes are introduced to remind us that we are dealing with a $\bar{b} \to \bar{s}c\bar{c}$ quark-level process. Using the unitarity of the CKM matrix, the $B^0_d \to J/\psi K^0_S$ decay amplitude can be expressed in the following form [9]:

$$A\left(B^0_d \to J/\psi K^0_S\right) = \left(1 - \frac{\lambda^2}{2}\right) \mathcal{A}' \left[1 + \epsilon a' e^{i\theta'} e^{i\gamma}\right], \tag{3.1}$$

where

$$\mathcal{A}' \equiv \lambda^2 A \left[C' + P'^{(c)} - P'^{(t)}\right] \tag{3.2}$$

and

$$a' e^{i\theta'} \equiv R_b \left[\frac{P'^{(u)} - P'^{(t)}}{C' + P'^{(c)} - P'^{(t)}}\right] \tag{3.3}$$

are CP-conserving hadronic parameters. The Wolfenstein parameter λ takes the value $\lambda \equiv |V_{us}| = 0.22551 \pm 0.00068$ [7], and

$$\epsilon \equiv \frac{\lambda^2}{1 - \lambda^2}, \qquad A \equiv \frac{|V_{cb}|}{\lambda^2}, \qquad R_b \equiv \left(1 - \frac{\lambda^2}{2}\right) \frac{1}{\lambda} \left|\frac{V_{ub}}{V_{cb}}\right| \tag{3.4}$$

are combinations of CKM matrix elements. The parameter a' measures the size of the penguin topologies with respect to the tree contribution, and is associated with the CP-conserving strong phase θ'. A key feature of the decay amplitude in eq. (3.1) is the suppression of the $a' e^{i\theta'} e^{i\gamma}$ term by the tiny factor $\epsilon = 0.0536 \pm 0.0003$. Consequently, ϕ_d can be extracted with the help of eq. (2.11) up to corrections of $\mathcal{O}(\epsilon a')$.

As was pointed out in ref. [9], the decay $B^0_s \to J/\psi K^0_S$ is related to $B^0_d \to J/\psi K^0_S$ through the U-spin symmetry of strong interactions. It originates from $\bar{b} \to \bar{d}c\bar{c}$ transitions and therefore has a CKM structure which is different from $B^0_d \to J/\psi K^0_S$. In analogy to eq. (3.1), we write

$$A\left(B^0_s \to J/\psi K^0_S\right) = -\lambda \mathcal{A} \left[1 - a e^{i\theta} e^{i\gamma}\right], \tag{3.5}$$

where the hadronic parameters are defined as their $B^0_d \to J/\psi K^0_S$ counterparts. In contrast to eq. (3.1), there is no ϵ factor present in front of the second term, thereby "magnifying"

the penguin effects. On the other hand, the λ in front of the overall amplitude suppresses the branching ratio with respect to $B_d^0 \to J/\psi K_S^0$.

The U-spin symmetry of strong interactions implies

$$a' e^{i\theta'} = a e^{i\theta} . \qquad (3.6)$$

In the factorisation approximation the hadronic form factors and decay constants cancel in the above amplitude ratios [9], i.e. U-spin-breaking corrections enter $ae^{i\theta}$ through non-factorisable effects only. On the other hand, the relation

$$\mathcal{A}' = \mathcal{A} \qquad (3.7)$$

is already in factorisation affected by SU(3)-breaking effects, entering through hadronic form factors as we will discuss in more detail below.

It is well known that the factorisation approximation does not reproduce the branching ratios of $B \to J/\psi K$ decays well, thereby requiring large non-factorisable effects. Furthermore, the QCD penguin matrix elements of the current-current tree operators, which are usually assumed to yield the potential enhancement for the penguin contributions, vanish in naive factorisation for $B \to J/\psi K$ decays. Consequently, large non-factorisable contributions may also affect the penguin parameters $a' e^{i\theta'}$ and $a e^{i\theta}$, thereby enhancing them from the smallish values in factorisation, and eq. (3.6) may receive sizeable corrections — despite the cancellation of form factors and decay constants in factorisation.

Making the replacements

$$B_s^0 \to J/\psi K_S^0 : b_f e^{i\rho_f} \to a e^{i\theta} , \qquad B_d^0 \to J/\psi K_S^0 : b_f e^{i\rho_f} \to -\epsilon a' e^{i\theta'} , \qquad (3.8)$$

we may apply the formalism introduced in section 2, yielding the following phase shifts:

$$\tan \Delta\phi_s^{\psi K^0} = \frac{-2a\cos\theta \sin\gamma + a^2 \sin 2\gamma}{1 - 2a\cos\theta \cos\gamma + a^2 \cos 2\gamma} = -2a\cos\theta \sin\gamma - a^2 \cos 2\theta \sin 2\gamma + \mathcal{O}(a^3) , \quad (3.9)$$

$$\tan \Delta\phi_d^{\psi K^0} = \frac{2\epsilon a' \cos\theta' \sin\gamma + \epsilon^2 a'^2 \sin 2\gamma}{1 + 2\epsilon a' \cos\theta' \cos\gamma + \epsilon^2 a'^2 \cos 2\gamma} = 2\epsilon a' \cos\theta' \sin\gamma + \mathcal{O}(\epsilon^2 a'^2) . \qquad (3.10)$$

The expansions in terms of the penguin parameters show an interesting feature: the phase shifts are maximal for a strong phase difference around $0°$ or $180°$. Conversely, the penguin shifts will be tiny for values around $90°$ or $270°$, even for sizeable $a^{(')}$. The $\Delta\phi_s^{\psi K^0}$ and $\Delta\phi_d^{\psi K^0}$ enter

$$\phi_{s,\psi K_S^0}^{\text{eff}} = \phi_s + \Delta\phi_s^{\psi K^0} , \qquad \phi_{d,\psi K_S^0}^{\text{eff}} = \phi_d + \Delta\phi_d^{\psi K^0} \qquad (3.11)$$

in the expressions corresponding to eq. (2.7). These "effective" mixing phases are convenient for the presentation of the experimental results [21].

3.2 Branching ratio information

The $B_s^0 \to J/\psi K_S^0$ decay channel has been observed by the CDF [24] and LHCb [25] collaborations, and measurements of the time-integrated untagged rate [26]

$$\mathcal{B}(B_s \to J/\psi K_S^0) \equiv \frac{1}{2} \int_0^\infty \langle \Gamma(B_s(t) \to J/\psi K_S^0) \rangle dt \qquad (3.12)$$

with
$$\langle\Gamma(B_s(t) \to J/\psi K_S^0)\rangle \equiv \Gamma(B_s^0(t) \to J/\psi K_S^0) + \Gamma(\bar{B}_s^0(t) \to J/\psi K_S^0) \tag{3.13}$$

were performed, resulting in the world average [27]
$$\mathcal{B}(B_s \to J/\psi K_S^0) = (1.87 \pm 0.17) \times 10^{-5} \,. \tag{3.14}$$

Information on the penguin parameters is also encoded in this observable, thereby complementing the CP asymmetries. In view of the sizeable decay width difference $\Delta\Gamma_s$ of the B_s-meson system, which is described by the parameter [28]
$$y_s \equiv \frac{\Delta\Gamma_s}{2\Gamma_s} = 0.0608 \pm 0.0045 \,, \tag{3.15}$$

the "experimental" branching ratio (3.12) has to be distinguished from the "theoretical" branching ratio defined by the untagged decay rate at time $t = 0$ [9]. The conversion of one branching ratio concept into the other can be done with the help of the following expression [29]:
$$\mathcal{B}\left(B_s \to J/\psi K_S^0\right)_{\text{theo}} = \left[\frac{1 - y_s^2}{1 + \mathcal{A}_{\Delta\Gamma}(B_s \to J/\psi K_S^0)\, y_s}\right] \mathcal{B}\left(B_s \to J/\psi K_S^0\right) \,. \tag{3.16}$$

The observable $\mathcal{A}_{\Delta\Gamma}(B_s \to J/\psi K_S^0)$ depends also on the penguin parameters, as can be seen in eq. (2.6).

The effective lifetime
$$\tau_{J/\psi K_S^0}^{\text{eff}} \equiv \frac{\int_0^\infty t\, \langle\Gamma(B_s(t) \to J/\psi K_S^0)\rangle\, dt}{\int_0^\infty \langle\Gamma(B_s(t) \to J/\psi K_S^0)\rangle\, dt} \tag{3.17}$$

$$= \frac{\tau_{B_s}}{1 - y_s^2} \left[\frac{1 + 2\mathcal{A}_{\Delta\Gamma}(B_s \to J/\psi K_S^0)\, y_s + y_s^2}{1 + \mathcal{A}_{\Delta\Gamma}(B_s \to J/\psi K_S^0)\, y_s}\right] \tag{3.18}$$

allows us to determine $\mathcal{A}_{\Delta\Gamma}(B_s \to J/\psi K_S^0)$, thereby fixing the conversion factor in eq. (3.16) [29]. The LHCb collaboration has performed the first measurement of this quantity [25]:
$$\tau_{J/\psi K_S^0}^{\text{eff}} = (1.75 \pm 0.12 \pm 0.07) \text{ ps} \,, \tag{3.19}$$

corresponding to
$$\mathcal{A}_{\Delta\Gamma}(B_s \to J/\psi K_S^0) = 2.1 \pm 1.6 \,. \tag{3.20}$$

In view of the large uncertainty of this measurement, we shall rely directly on eq. (2.6) with eq. (3.8) in the numerical analysis performed in section 3.4.

In order to utilise the branching ratio information, we construct the observable
$$H \equiv \frac{1}{\epsilon} \left|\frac{\mathcal{A}'}{\mathcal{A}}\right|^2 \frac{\text{PhSp}\left(B_d \to J/\psi K_S^0\right)}{\text{PhSp}\left(B_s \to J/\psi K_S^0\right)} \frac{\tau_{B_d}}{\tau_{B_s}} \frac{\mathcal{B}\left(B_s \to J/\psi K_S^0\right)_{\text{theo}}}{\mathcal{B}\left(B_d \to J/\psi K_S^0\right)_{\text{theo}}} \,, \tag{3.21}$$

where τ_{B_q} is the B_q lifetime and $\text{PhSp}\left(B_q \to J/\psi X\right)$ denotes the phase-space function for these decays [9]. In terms of the penguin parameters, we obtain
$$H = \frac{1 - 2\, a \cos\theta \cos\gamma + a^2}{1 + 2\epsilon a' \cos\theta' \cos\gamma + \epsilon^2 a'^2} = -\frac{1}{\epsilon} \frac{\mathcal{A}_{\text{CP}}^{\text{dir}}(B_d \to J/\psi K_S)}{\mathcal{A}_{\text{CP}}^{\text{dir}}(B_s \to J/\psi K_S)}, \tag{3.22}$$

where we also give the relation to the direct CP asymmetries of the decays at hand. Keeping a and θ as free parameters, the following lower bound arises [30, 31]:

$$H \geq \frac{1 + \epsilon^2 + 2\epsilon \cos^2 \gamma - (1 + \epsilon)\sqrt{1 - 2\epsilon + \epsilon^2 + 4\epsilon \cos^2 \gamma}}{2\epsilon^2 (1 - \cos^2 \gamma)}, \qquad (3.23)$$

which corresponds to $H \geq 0.872$ for $\gamma = 70°$.

The determination of H from the experimentally measured branching ratios is affected by U-spin-breaking corrections which enter through the ratio $|\mathcal{A}'/\mathcal{A}|$. Consequently, H is not a particularly clean observable. On the other hand, the analysis of the direct and mixing-induced CP asymmetries does not require knowledge of $|\mathcal{A}'/\mathcal{A}|$.

3.3 Determination of γ and the penguin parameters

If we complement the ratio H with the direct and mixing-induced CP asymmetries of the $B_s^0 \to J/\psi K_S^0$ channel, we have sufficient information to determine γ and the penguin parameters a and θ by means of the U-spin relation in eq. (3.6) [9]. In this strategy, ϕ_s serves as an input, where we may either use its SM value in eq. (1.2) or the value extracted from experimental data, as discussed in section 4. We advocate the latter option since it takes possible CP-violating NP contributions to B_s^0-$\bar{B}_s^0$ mixing into account.

Although γ can be extracted with this method at the LHCb upgrade, the corresponding precision is not expected to be competitive with other strategies [32]. It is therefore advantageous to employ γ as an input. Using data from pure tree decays of the kind $B \to D^{(*)}K^{(*)}$, the following averages were obtained by the CKMfitter and UTfit collaborations:

$$\gamma = (70.0^{+7.7}_{-9.0})° \quad \text{(CKMfitter [7])}, \qquad \gamma = (68.3 \pm 7.5)° \quad \text{(UTfit [33])}. \qquad (3.24)$$

For the numerical analysis in this paper, we shall use the CKMfitter result in view of the larger uncertainty. By the time of the LHCb upgrade and Belle II era, much more precise measurements of γ from pure tree decays will be available (see section 3.5).

Once the direct and mixing-induced CP asymmetries of the $B_s^0 \to J/\psi K_S^0$ channel have been measured, eqs. (2.4) and (2.5) can be used with eq. (3.8) to determine a and θ in a theoretically clean way. Employing the U-spin relation (3.6) allows us to convert these parameters into the phase shift $\Delta\phi_d^{\psi K_S^0}$, and thus to include the penguin effects in the determination of ϕ_d.

3.4 Constraining the penguin effects through current data

As a measurement of CP violation in $B_s^0 \to J/\psi K_S^0$ is not yet available, the U-spin strategy sketched above cannot yet be implemented in practice. However, in order to already obtain information on the size of the penguin parameters a and θ and their impact on high-precision studies of CP violation, we may use experimental data for decays which have dynamics similar to $B_s^0 \to J/\psi K_S^0$.

If we replace the strange spectator quark with a down quark, as proposed in ref. [10], we obtain the $B_d^0 \to J/\psi \pi^0$ decay [12, 13], which is the vector–pseudo-scalar counterpart of the vector–vector mode $B_d^0 \to J/\psi \rho^0$. The $B_d^0 \to J/\psi \pi^0$ mode has contributions from penguin
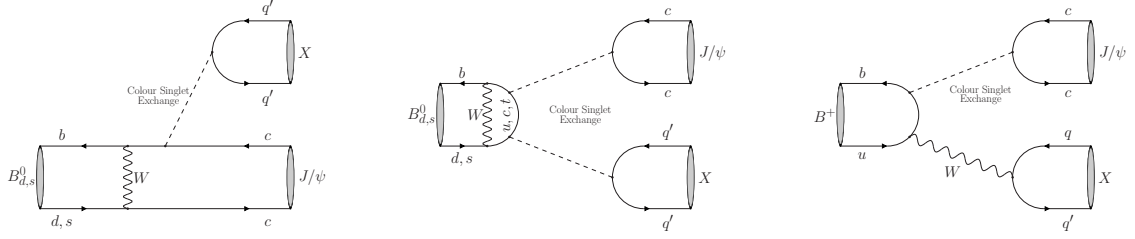
Figure 2. Illustration of additional decay topologies contributing to some of the $B \to J/\psi X$ channels: exchange (left), penguin annihilation (middle) and annihilation (right).

annihilation and exchange topologies, illustrated in figure 2, which have no counterpart in $B_s^0 \to J/\psi K_S^0$ and are expected to be small. They can be probed through the $B_s^0 \to J/\psi \pi^0$ decay (and $B_s^0 \to J/\psi \rho^0$ for $B_d^0 \to J/\psi \rho^0$) [14]. First measurements of CP violation in $B_d^0 \to J/\psi \pi^0$ were reported by the BaBar and Belle collaborations:

$$\mathcal{A}_{\text{CP}}^{\text{dir}}(B_d \to J/\psi \pi^0) = \begin{cases} -0.08 \pm 0.16 \pm 0.05 & \text{(Belle [34])} \\ -0.20 \pm 0.19 \pm 0.03 & \text{(BaBar [35])} \end{cases} \tag{3.25}$$

$$\mathcal{A}_{\text{CP}}^{\text{mix}}(B_d \to J/\psi \pi^0) = \begin{cases} 0.65 \pm 0.21 \pm 0.05 & \text{(Belle [34])} \\ 1.23 \pm 0.21 \pm 0.04 & \text{(BaBar [35])}. \end{cases} \tag{3.26}$$

The results for the mixing-induced CP asymmetry are not in good agreement with each other, with the BaBar result lying outside the physical region. The Heavy Flavour Averaging Group (HFAG) has refrained from inflating the uncertainties in their average, giving $\mathcal{A}_{\text{CP}}^{\text{mix}}(B_d \to J/\psi \pi^0) = 0.93 \pm 0.15$ [28]. The Belle II experiment will hopefully clarify this unsatisfactory situation.

The charged counterpart $B^+ \to J/\psi \pi^+$ of $B_d^0 \to J/\psi \pi^0$ also has dynamics similar to $B_s^0 \to J/\psi K_S^0$ but — as it is the decay of a charged B meson — does not exhibit mixing-induced CP violation. It receives additional contributions from an annihilation topology, illustrated in figure 2, which arises with the same CKM factor $V_{ud}V_{ub}^*$ as the penguin topologies with internal up-quark exchanges, contributing similarly to the penguin parameter $a_c e^{i\theta_c}$ (defined in analogy to eq. (3.3)). If this parameter is determined from the charged $B^+ \to J/\psi \pi^+$, $B^+ \to J/\psi K^+$ decays and compared with the other penguin parameters, footprints of the annihilation topology could be detected. In view of the present uncertainties, we neglect the annihilation topology, like the contributions from the exchange and penguin annihilation topologies in $B_d^0 \to J/\psi \pi^0$. In appendix A, we give a more detailed discussion of the annihilation contribution and its importance based on constraints from current data, which do not indicate any enhancement.

We shall also add data for the $B^+ \to J/\psi K^+$ (neglecting again the corresponding annihilation contribution) and $B_d^0 \to J/\psi K^0$ modes to the global analysis, although the penguin contributions are doubly Cabibbo-suppressed in these decays.

Using the SU(3) flavour symmetry and assuming both vanishing non-factorisable corrections and vanishing exchange and annihilation topologies, the decays listed above are characterised by a universal set of penguin parameters (a, θ), which can be extracted from
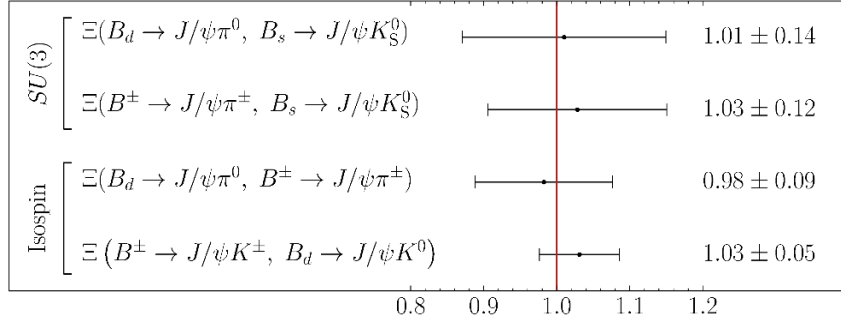
Figure 3. Overview of the different ratios defined in eq. (3.27). In the limit where we neglect the contributions from additional decay topologies and assume perfect flavour symmetry for the spectator quarks, the ratios equal unity.
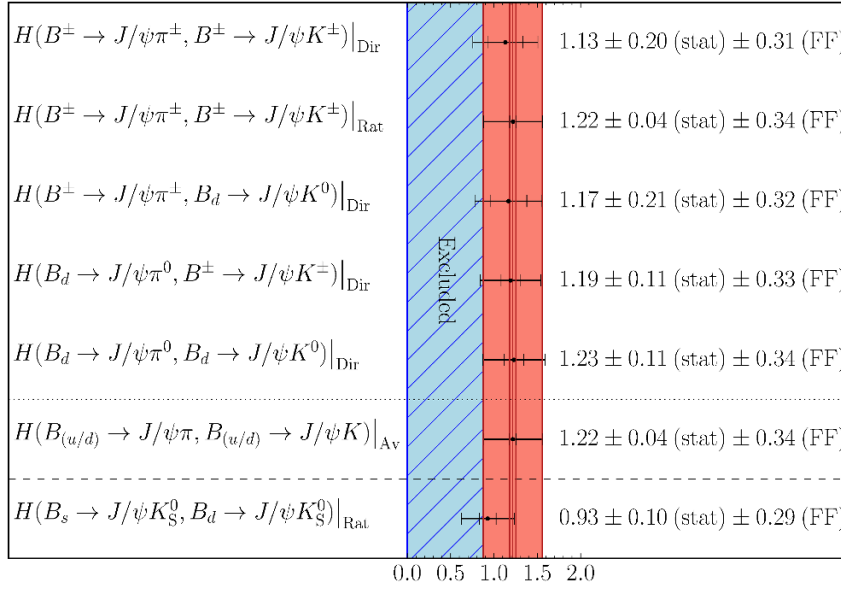

Figure 4. H observables which can be constructed from the available branching ratio information for $B_q \to J/\psi P$ modes. The label "Dir" indicates that H is determined from direct branching fraction measurements, whereas the label "Rat" is used for H observables calculated from a ratio of branching fractions. The inner uncertainty bars indicate the statistical uncertainty whereas the outer ones give the total uncertainty, including the common uncertainty due to the form factors. The red band indicates the average H observable of the $B_{(u/d)} \to J/\psi(\pi/K)$ modes. The hatched blue region is excluded by eq. (3.23).

the input data through a global χ^2 fit. The resulting picture extends and updates the previous analyses of refs. [12–14].

A first consistency check is provided by the ratios

$$\Xi(B_q \to J/\psi X, B_{q'} \to J/\psi Y) \equiv \frac{\text{PhSp}\left(B_{q'} \to J/\psi Y\right)}{\text{PhSp}\left(B_q \to J/\psi X\right)} \frac{\tau_{B_{q'}}}{\tau_{B_q}} \frac{\mathcal{B}\left(B_q \to J/\psi X\right)_{\text{theo}}}{\mathcal{B}\left(B_{q'} \to J/\psi Y\right)_{\text{theo}}}, \quad (3.27)$$

involving decays which originate from the same quark-level processes but differ through their spectator quarks [32]. Neglecting exchange and annihilation topologies and assuming

perfect flavour symmetry of strong interactions, these ratios equal one. Within the uncertainties, this picture is supported by the data, as shown in figure 3. In this compilation, the B-factory branching ratio measurements are corrected for the measured pair production asymmetry between $B_d^0 \bar{B}_d^0$ and $B^+ B^-$ [27] at the $\Upsilon(4S)$ resonance. Note that the branching ratios for decays into final states with K_S^0 or π^0 mesons have to be multiplied by a factor of two in eq. (3.27) to take the K_S^0 and π^0 wave functions into account.

Let us now probe the penguin parameters through the various branching ratios. To this end, we use ratios defined in analogy to H in eq. (3.21). The extraction of these quantities from the data requires knowledge of the amplitude ratio $|\mathcal{A}'/\mathcal{A}|$, which is given in factorisation as follows [9]:

$$\left| \frac{\mathcal{A}'(B_{q'} \to J/\psi X)}{\mathcal{A}(B_q \to J/\psi Y)} \right|_{\text{fact}} = \frac{f_{B_{q'} \to X}^+(m_{J/\psi}^2)}{f_{B_q \to Y}^+(m_{J/\psi}^2)} \, . \tag{3.28}$$

The corresponding form factors have been calculated in the literature using a variety of techniques. For our analysis, we take the results from light cone QCD sum rules (LCSR), which are typically calculated at $q^2 = 0$. The relevant form factors are $f_{B \to \pi}^+(0) = 0.252_{-0.028}^{+0.019}$ [36], $f_{B \to K}^+(0) = 0.34_{-0.02}^{+0.05}$ [37] and $f_{B_s \to K}^+(0) = 0.30_{-0.03}^{+0.04}$ [38], where the first two describe transitions for both the B_d^0 and the B^+ mesons. The q^2 dependence of these form factors is parametrised by means of the BGL method described in ref. [39].

Using these form factors and neglecting non-factorisable SU(3)-breaking effects, we obtain the various H observables compiled in figure 4. With exception of the last entry, all H observables share the same ratio $f_{B \to K}^+/f_{B \to \pi}^+$. Consequently, their central values and uncertainties are highly correlated. However, even restricting the comparison to the statistical uncertainties shows an excellent compatibility between the various H results. The corresponding ratios are related to each other through the isospin symmetry (neglecting additional topologies), and we obtain a consistent experimental picture. The agreement with the last entry, which involves the decay $B_s^0 \to J/\psi K_S^0$ instead of the $B \to J/\psi \pi$ modes, suggests that non-factorisable SU(3)-breaking effects and the impact of additional decay topologies are small, thereby complementing the picture of figure 3. The uncertainties are still too large to draw definite conclusions.

For the global χ^2 fit to extract the penguin parameters a and θ we use the input quantities summarised in table 1, and add the CKMfitter result for γ in eq. (3.24) as an asymmetric Gaussian constraint. As far as the H observables are concerned, we employ the average of the $B_{(u/d)} \to J/\psi(\pi/K)$ combinations, which involve the same set of form factors (see figure 4), and the H observable of the $B_{s,d}^0 \to J/\psi K_S^0$ system. The branching ratios entering the H observables are complemented by the corresponding direct CP asymmetries.

In order to add the mixing-induced CP asymmetry of the $B_d^0 \to J/\psi \pi^0$ channel to the fit, the B_d^0-$\bar{B}_d^0$ mixing phase ϕ_d is needed as an input. However, the measured CP-violating asymmetries of the $B_d^0 \to J/\psi K_S^0$ decay allow us to determine only the effective mixing

Observable	Experimental result	
$\mathcal{A}_{\mathrm{CP}}^{\mathrm{dir}}(B^{\pm} \to J/\psi\pi^{\pm})$	-0.001 ± 0.023	[27]
$\mathcal{A}_{\mathrm{CP}}^{\mathrm{dir}}(B_d \to J/\psi\pi^0)$	-0.13 ± 0.13	[27]
$\mathcal{A}_{\mathrm{CP}}^{\mathrm{mix}}(B_d \to J/\psi\pi^0)$	0.94 ± 0.15	[27]
$\mathcal{A}_{\mathrm{CP}}^{\mathrm{dir}}(B^{\pm} \to J/\psi K^{\pm})$	-0.0030 ± 0.0033	[27]
$\mathcal{A}_{\mathrm{CP}}^{\mathrm{dir}}(B_d \to J/\psi K^0)$	0.007 ± 0.020	[28]
$\mathcal{A}_{\mathrm{CP}}^{\mathrm{mix}}(B_d \to J/\psi K^0)$	-0.670 ± 0.021	[28]
$H(B_{(u/d)} \to J/\psi(\pi/K))$	1.22 ± 0.34	Figure 4
$H(B_{(s/d)} \to J/\psi K_{\mathrm{S}}^0)$	0.93 ± 0.31	Figure 4

Table 1. Input quantities for the global χ^2 fit to the penguin parameters a, θ and ϕ_d.

phase[2]

$$\phi_{d,\psi K_{\mathrm{S}}^0}^{\mathrm{eff}} = \phi_d + \Delta\phi_d^{\psi K_{\mathrm{S}}^0} = (42.1 \pm 1.6)^{\circ} \tag{3.29}$$

from eq. (2.7). But — if we express the phase shift $\Delta\phi_d^{\psi K_{\mathrm{S}}^0}$ in terms of the penguin parameters — we may add this observable to our analysis.

The global fit yields $\chi_{\mathrm{min}}^2 = 2.6$ for four degrees of freedom $(a, \theta, \phi_d, \gamma)$, indicating good agreement between the different input quantities. It results in the solutions

$$a = 0.19_{-0.12}^{+0.15}, \qquad \theta = (179.5 \pm 4.0)^{\circ} \tag{3.30}$$

and

$$\phi_d = \left(43.2_{-1.7}^{+1.8}\right)^{\circ}, \tag{3.31}$$

while γ is constrained to the input in eq. (3.24). In figure 5, we show the correlation between ϕ_d and a. The value of ϕ_d in eq. (3.31) will serve as an input in section 4. Following ref. [14], we illustrate the various constraints entering the fit through contour bands of the individual observables in figure 6. For the $\mathcal{A}_{\mathrm{CP}}^{\mathrm{mix}}(B_d \to J/\psi\pi^0)$ range, we have used the value of ϕ_d in eq. (3.31). In comparison with the analysis of ref. [14], the penguin parameters are now constrained in a more stringent way. The penguin parameters in eq. (3.30) result in the following penguin phase shift:

$$\Delta\phi_d^{\psi K_{\mathrm{S}}^0} = -\left(1.10_{-0.85}^{+0.70}\right)^{\circ}, \tag{3.32}$$

with confidence level contours shown in figure 7.

3.5 Benchmark scenario for $B_{d,s}^0 \to J/\psi K_{\mathrm{S}}^0$

Let us conclude the analysis of the penguin effects in $B_d^0 \to J/\psi K_{\mathrm{S}}^0$ by discussing a future benchmark scenario pointing to the LHCb upgrade era. Using the results in eq. (3.30) and assuming the SM value for ϕ_s in eq. (1.2), we obtain the following predictions:

$$\mathcal{A}_{\Delta\Gamma}(B_s \to J/\psi K_{\mathrm{S}}^0) = 0.957 \pm 0.061, \tag{3.33}$$

---

[2]The numerical value in eq. (3.29) actually corresponds to the mixing-induced CP asymmetry $\mathcal{A}_{\mathrm{CP}}^{\mathrm{mix}}(B_d \to J/\psi K^0)$, which is an average of $B_d^0 \to J/\psi K_{\mathrm{S}}^0$ and $B_d^0 \to J/\psi K_{\mathrm{L}}^0$ data [28].
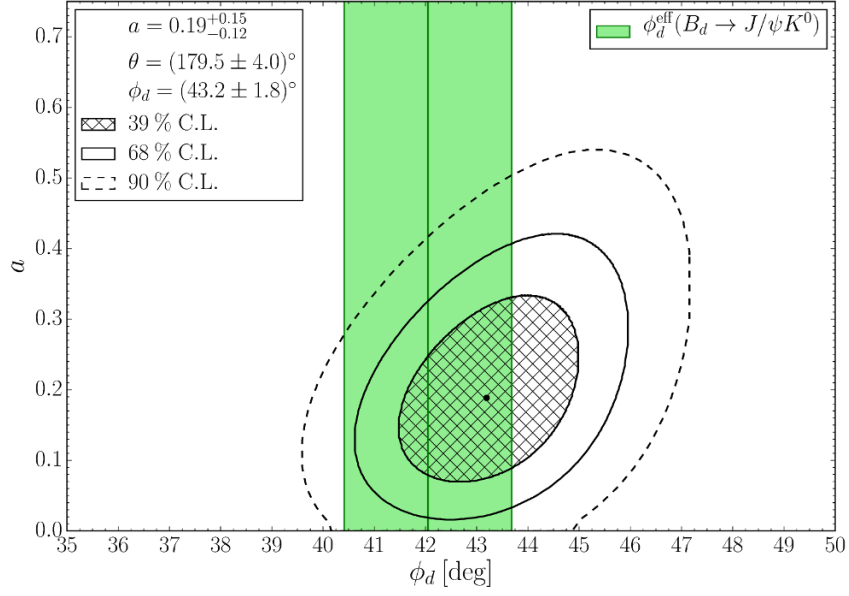
Figure 5. Correlation between the B_d^0-$\bar{B}_d^0$ mixing phase ϕ_d and the penguin parameter a arising from the χ^2 fit to current data as described in the text.
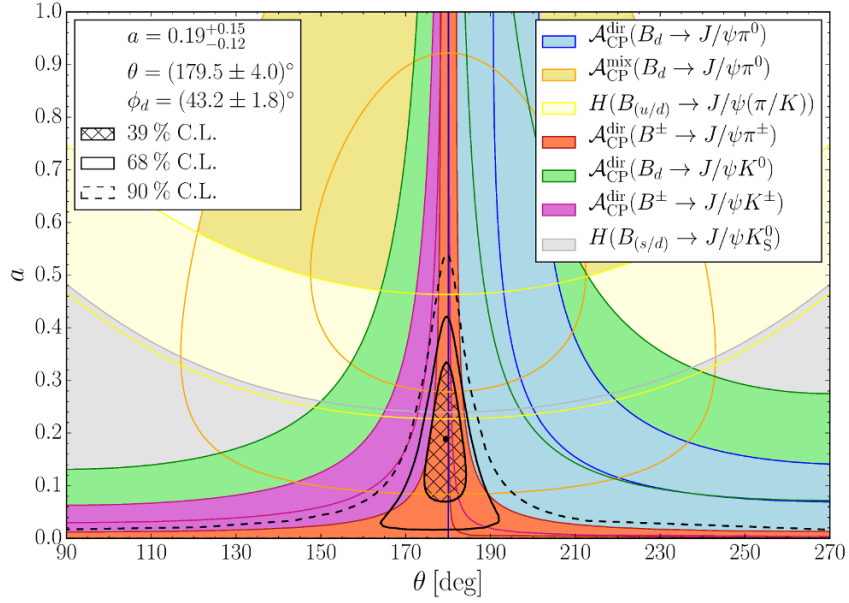

Figure 6. Determination of the penguin parameters a and θ through intersecting contours derived from CP asymmetries and branching ratios of $B_q \to J/\psi P$ decays. We show also the confidence level contours obtained from a χ^2 fit to the data. To improve the visualisation, the allowed range for a has been extended to 1.
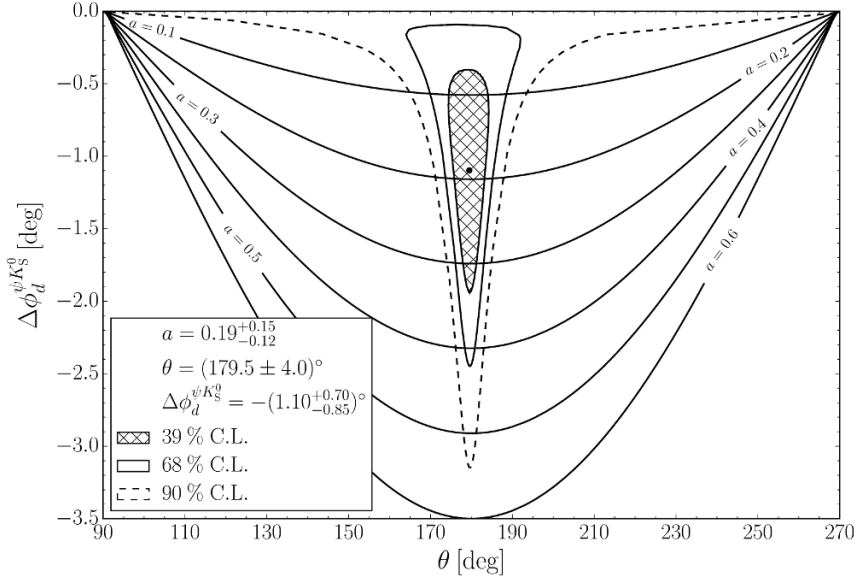
– 13 –

Figure 7. Constraints on $\Delta\phi_d^{\psi K_S^0}$ as a function of the strong phase θ arising from the χ^2 fit to the data. Superimposed are the contour levels for the penguin parameter a.
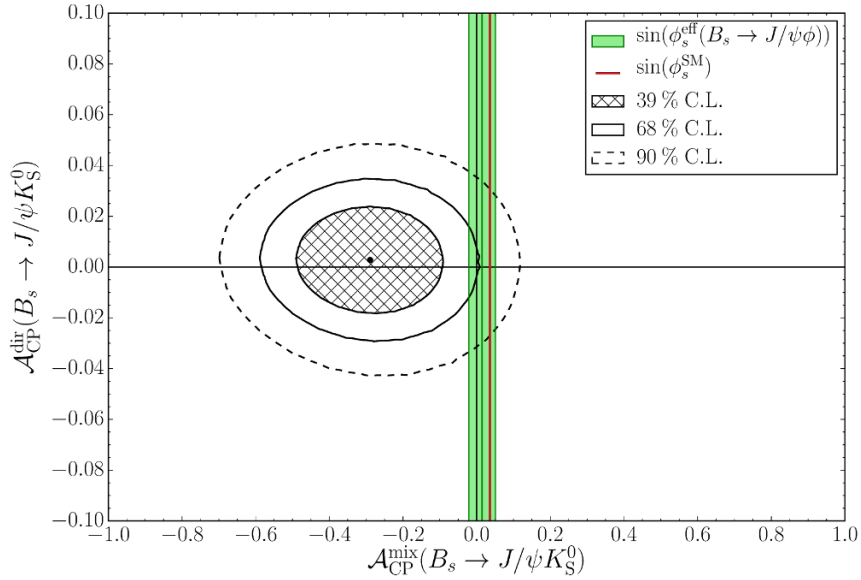

Figure 8. Prediction of CP violation in $B_s^0 \to J/\psi K_S^0$ following from the global χ^2 fit to the present data as discussed in section 3.4.

$$\mathcal{A}_{\text{CP}}^{\text{dir}}(B_s \to J/\psi K_S^0) = 0.003 \pm 0.021 \, , \tag{3.34}$$

$$\mathcal{A}_{\text{CP}}^{\text{mix}}(B_s \to J/\psi K_S^0) = -0.29 \pm 0.20 \, . \tag{3.35}$$

The associated confidence level contours for $\mathcal{A}_{\text{CP}}^{\text{dir}}(B_s \to J/\psi K_S^0)$ and $\mathcal{A}_{\text{CP}}^{\text{mix}}(B_s \to J/\psi K_S^0)$ are shown in figure 8. Moreover, the penguin parameters in eq. (3.30) yield

$$\tau_{J/\psi K_S^0}^{\text{eff}} = (1.603 \pm 0.010) \text{ ps} \, , \tag{3.36}$$

in agreement with the experimental result in eq. (3.19).

In order to illustrate the potential of the $B_s^0 \to J/\psi K_S^0$ decay to extract the penguin parameters at the LHCb upgrade, let us assume that γ has been determined in a clean way from pure tree decays $B \to D^{(*)} K^{(*)}$ as

$$\gamma = (70 \pm 1)^\circ \, , \tag{3.37}$$

and that the B_s^0-$\bar{B}_s^0$ mixing phase has been extracted from the $B_s^0 \to J/\psi \phi$ angular analysis and the application of the strategies discussed in sections 4 and 5 to control the penguin effects as

$$\phi_s = - (2.1 \pm 0.5|_{\text{exp}} \pm 0.3|_{\text{theo}})^\circ = -(2.1 \pm 0.6)^\circ \, . \tag{3.38}$$

The experimental uncertainty projections for the LHCb upgrade are discussed in ref. [40]. We consider our assessment of the theoretical uncertainty of ϕ_s in eq. (3.38) as conservative.

Let us assume that the CP-violating asymmetries of the $B_s^0 \to J/\psi K_S^0$ channel have been measured as follows:

$$\mathcal{A}_{\text{CP}}^{\text{dir}}(B_s \to J/\psi K_S^0) = 0.00 \pm 0.05 \, , \qquad \mathcal{A}_{\text{CP}}^{\text{mix}}(B_s \to J/\psi K_S^0) = -0.28 \pm 0.05 \, , \tag{3.39}$$

i.e. with the central values of eqs. (3.34) and (3.35). In order to estimate the uncertainties, current LHCb measurements of CP violation in $B_s^0 \to D_s^\mp K^\pm$ modes [41] have been extrapolated to the LHCb upgrade era, correcting for the $B_s^0 \to J/\psi K_S^0$ event yield [42].

A χ^2 fit to these observables would then yield

$$a = 0.189^{+0.034}_{-0.032} \, , \qquad \theta = (179.5 \pm 9.4)^\circ \, . \tag{3.40}$$

The corresponding confidence level contours are shown in figure 9.

In contrast to the fit in figure 6, this "future" determination of a and θ is theoretically clean. Using the U-spin relation (3.6), these parameters can be converted into the penguin phase shift of $B_d^0 \to J/\psi K_S^0$. It is only at this point that potential U-spin-breaking effects enter. They can be included by introducing parameters ξ and δ as follows:

$$a' = \xi \cdot a \, , \qquad \theta' = \theta + \delta \, . \tag{3.41}$$

Assuming $\xi = 1.00 \pm 0.20$ and $\delta = (0 \pm 20)^\circ$, the results for a and θ in figure 9 yield

$$\Delta\phi_d^{\psi K_S^0} = - \left[1.09 \pm 0.20 \, (\text{stat})^{+0.20}_{-0.24} \, (\text{U-spin}) \right]^\circ \, , \tag{3.42}$$

with the corresponding contours shown in figure 10. In this benchmark scenario, the experimental and theoretical uncertainties are of the same size, with a total uncertainty of
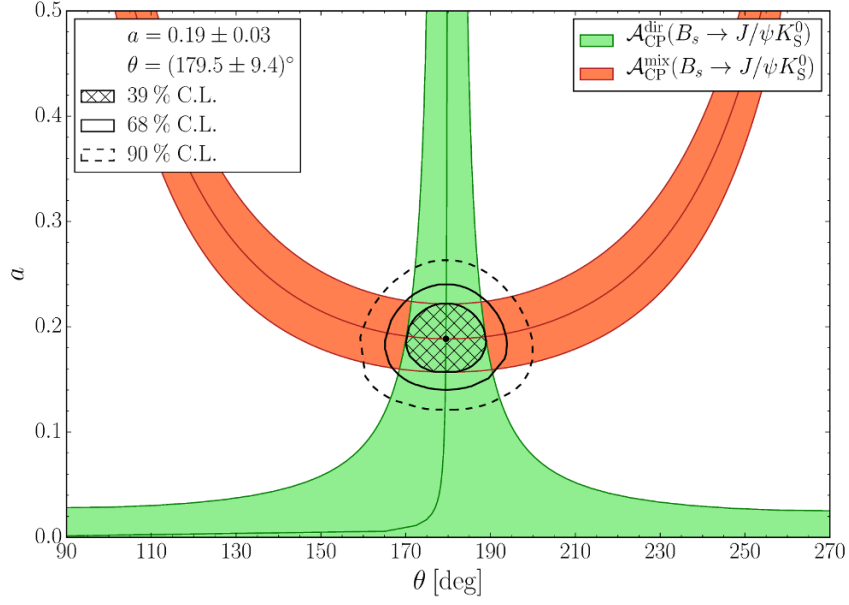
Figure 9. Benchmark scenario illustrating the determination of the penguin parameters a and θ from the CP asymmetries of the $B_s^0 \to J/\psi K_S^0$ decay.
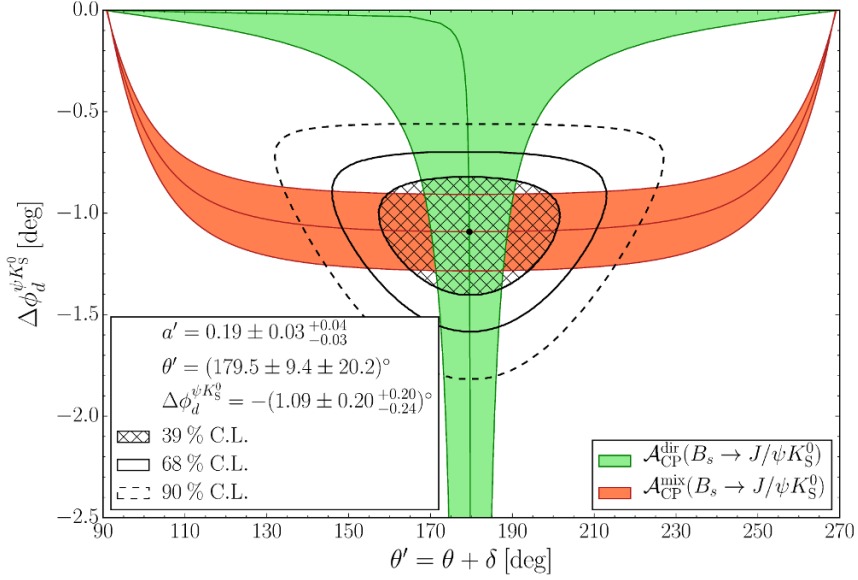

Figure 10. Benchmark scenario illustrating the determination of $\Delta\phi_d^{\psi K_S^0}$ from the CP asymmetries of the $B_s^0 \to J/\psi K_S^0$ decay. The confidence level contours assume a 20% uncertainty for U-spin breaking effects, parametrised through eq. (3.41).

0.3° if added in quadrature. By the time such measurements will be available, we should have better experimental insights into U-spin-breaking effects. As we will see in section 4.3, already the currently available data for $B_d^0 \to J/\psi \rho^0$ decays do not favour large effects in the $B_d^0 \to J/\psi \rho^0$, $B_s^0 \to J/\psi \phi$ system.

It is important to emphasise that the observable H is *not* required in this analysis. Assuming eq. (3.6), it can rather be determined with the help of eq. (3.22). As a' enters there in combination with the tiny ϵ factor, the U-spin-breaking corrections have a negligible effect in this case. Using eq. (3.40), we obtain

$$H_{(a,\theta)} = 1.172 \pm 0.037 \, (a, \theta) \pm 0.0016 \, (\xi, \delta) \,. \tag{3.43}$$

The comparison with eq. (3.21) then allows us to extract the ratio

$$\left| \frac{\mathcal{A}'}{\mathcal{A}} \right| = \sqrt{\epsilon \, H_{(a,\theta)} \frac{\mathrm{PhSp}\left(B_s \to J/\psi K_S^0\right)}{\mathrm{PhSp}\left(B_d \to J/\psi K_S^0\right)} \frac{\tau_{B_s}}{\tau_{B_d}} \frac{\mathcal{B}\left(B_d \to J/\psi K_S^0\right)_{\mathrm{theo}}}{\mathcal{B}\left(B_s \to J/\psi K_S^0\right)_{\mathrm{theo}}}} \,. \tag{3.44}$$

In order to illustrate the corresponding future experimental precision, we use the central values of the penguin parameters in eq. (3.40) and combine them with information on the ratio of branching fractions. The systematic uncertainty of all B_s branching ratio measurements is limited by the ratio $f_s/f_d = 0.259 \pm 0.015$ [43, 44] of fragmentation functions, which is required for normalisation purposes [45]. At the LHCb upgrade, the experimental precision of the ratio of branching fractions entering eq. (3.44) will be governed by that of f_s/f_d. Assuming no further improvement in the determination of this parameter, which is conservative, would result in the measurement

$$\left| \frac{\mathcal{A}'}{\mathcal{A}} \right|_{\mathrm{exp}} = 1.160 \pm 0.035 \,. \tag{3.45}$$

The experimental uncertainty is about five times smaller than the current theoretical uncertainty of the factorisation result

$$\left| \frac{\mathcal{A}'}{\mathcal{A}} \right|_{\mathrm{fact}} = 1.16 \pm 0.18 \tag{3.46}$$

using LCSR form factors (see the discussion of eq. (3.28)). Consequently, the experimental determination of $|\mathcal{A}'/\mathcal{A}|$ is yet another interesting topic for the LHCb upgrade. It will provide valuable insights into possible non-factorisable U-spin-breaking effects and the hadronisation dynamics of the $B_{s,d}^0 \to J/\psi K_S^0$ system.

4 B decays into two vector mesons

4.1 Preliminaries

In the case of the $B_s^0 \to J/\psi \phi$ and $B_d^0 \to J/\psi \rho^0$ modes, the final states are mixtures of CP-even and CP-odd eigenstates. For the analysis of CP violation, these states have to be disentangled with the help of a time-dependent angular analysis of the $J/\psi \to \ell^+ \ell^-$ and $\phi \to K^+ K^-$, $\rho^0 \to \pi^+ \pi^-$ decay products [18, 19]. To this end, it is convenient to introduce

linear polarisation amplitudes $A_0(t)$, $A_\|(t)$ and $A_\perp(t)$ [46], where the 0 and $\|$ final state configurations are CP-even while $\perp$ describes a CP-odd state. A detailed discussion of the general structure of the various observables provided by the angular distribution in the presence of the penguin contributions was given in ref. [10]. The linear polarisation states are also employed for the theoretical description of the $B_s^0 \to J/\psi \bar{K}^{*0}$ decay, which has a flavour-specific final state [15].

4.2   The $B_s^0 \to J/\psi\phi$ channel

The decay $B_s^0 \to J/\psi\phi$ is the B_s^0-meson counterpart of $B_d^0 \to J/\psi K_S^0$. Assuming that the ϕ meson is a pure $s\bar{s}$ state, i.e. neglecting ω-ϕ mixing (for a detailed discussion, see ref. [15]), this transition arises if we replace the down spectator quark of $B_d^0 \to J/\psi K_S^0$ by a strange quark. In analogy to eq. (3.1), the SM decay amplitude takes the following form [10, 15]:

$$A\left(B_s^0 \to (J/\psi\phi)_f\right) = \left(1 - \frac{\lambda^2}{2}\right) \mathcal{A}'_f \left[1 + \epsilon a'_f e^{i\theta'_f} e^{i\gamma}\right] , \qquad (4.1)$$

where the label $f \in \{0, \|, \perp\}$ distinguishes between the different configurations of the final state vector mesons. We have to make the replacements

$$B_s^0 \to J/\psi\phi : b_f e^{i\rho_f} \to -\epsilon a'_f e^{i\theta'_f} , \qquad \mathcal{N}_f \to \left(1 - \frac{\lambda^2}{2}\right) \mathcal{A}'_f \qquad (4.2)$$

in order to apply the formalism introduced in section 2. The hadronic phase shift

$$\phi_{s,(\psi\phi)_f}^{\text{eff}} = \phi_s + \Delta\phi_s^{(\psi\phi)_f} \qquad (4.3)$$

can be obtained from eq. (2.10).

The penguin parameters (a'_f, θ'_f) are — in general — expected to differ for different final-state configurations f. However, applying simplified arguments along the lines of factorisation, the following picture emerges [10]:

$$a'_f \equiv a'_{\psi\phi} , \qquad \theta'_f \equiv \theta'_{\psi\phi} \qquad \forall f \in \{0, \|, \perp\} . \qquad (4.4)$$

The reason giving rise to the polarisation-independent parameters is the feature that form factors, which may depend on the final-state configuration f, cancel in the a'_f ratios of penguin to tree amplitudes. It is an interesting question to test eq. (4.4) with experimental data, in particular in view of the discussion in the paragraph after eqs. (3.6) and (3.7). The parameters $a'_{\psi\phi}$ and $\theta'_{\psi\phi}$ in eq. (4.4) may differ from their $B_d^0 \to J/\psi K_S^0$ counterparts in eq. (3.1) due to the different hadronisation dynamics and non-factorisable effects.

The LHCb collaboration has recently presented the first results for the effective B_s^0-$\bar{B}_s^0$ mixing phases for the different final-state polarisations [20]:

$$\phi_{s,0}^{\text{eff}} = -0.045 \pm 0.053 \pm 0.007 = -(2.58 \pm 3.04 \pm 0.40)^\circ , \qquad (4.5)$$

$$\phi_{s,\|}^{\text{eff}} - \phi_{s,0}^{\text{eff}} = -0.018 \pm 0.043 \pm 0.009 = -(1.03 \pm 2.46 \pm 0.52)^\circ , \qquad (4.6)$$

$$\phi_{s,\perp}^{\text{eff}} - \phi_{s,0}^{\text{eff}} = -0.014 \pm 0.035 \pm 0.006 = -(0.80 \pm 2.01 \pm 0.34)^\circ . \qquad (4.7)$$

Within the uncertainties, no dependence on the final-state configuration is revealed. Moreover, eq. (4.5) is in excellent agreement with the SM value in eq. (1.2). Using eq. (3.32) as a guideline for the size of possible hadronic phase shifts in $B_s^0 \to J/\psi\phi$, the current precision is not yet high enough for resolving such effects. However, the LHCb analysis of ref. [20] has a pioneering character, and it will be very interesting to monitor the polarisation-dependent measurements as the precision increases. Assuming a universal value of ϕ_s^{eff}, i.e. the relations in eq. (4.4), the following result is obtained from the time-dependent analysis of the $B_s^0 \to J/\psi[\to \mu^+\mu^-]\phi[\to K^+K^-]$ angular distribution [20]:

$$\phi_s^{\mathrm{eff}} = \phi_s + \Delta\phi_s = -0.058 \pm 0.049 \pm 0.006 = -(3.32 \pm 2.81 \pm 0.34)^\circ . \qquad (4.8)$$

The LHCb collaboration has also reported first polarisation-dependent results for the following quantities:

$$|\lambda_f| \equiv \left| \frac{A(\bar{B}_s^0 \to (J/\psi\phi)_f)}{A(B_s^0 \to (J/\psi\phi)_f)} \right| = \left| \frac{1 + \epsilon a_f' e^{i\theta_f'} e^{-i\gamma}}{1 + \epsilon a_f' e^{i\theta_f'} e^{+i\gamma}} \right| . \qquad (4.9)$$

In this expression, CP violation in B_s^0-$\bar{B}_s^0$ oscillations, which is a tiny effect [47], has been neglected, like in eq. (2.3) with eqs. (2.4), (2.5) and (2.6). The LHCb measurements are given by

$$|\lambda^0| = 1.012 \pm 0.058 \pm 0.013 , \qquad (4.10)$$

$$|\lambda^\perp/\lambda^0| = 1.02 \pm 0.12 \pm 0.05 , \qquad (4.11)$$

$$|\lambda^\parallel/\lambda^0| = 0.97 \pm 0.16 \pm 0.01 . \qquad (4.12)$$

Within the current uncertainties, again no polarisation dependence is observed. This is in agreement with the structure of eq. (4.9), where the parameter $a_f' e^{i\theta_f'}$ enters with $\epsilon \sim 0.05$. If we use the fit result in eq. (3.30) as a guideline and assume $a_f' e^{i\theta_f'} \sim 0.2$, we obtain $|\lambda^f| = 1 + \mathcal{O}(0.01)$, which sets the scale of the required precision to resolve possible footprints of the penguin contributions in these measurements.

Assuming that the parameters $|\lambda^f| \equiv |\lambda_{\psi\phi}|$ do not depend on the final-state configuration of the vector mesons, the LHCb collaboration has extracted the following result from the $B_s^0 \to J/\psi[\to \mu^+\mu^-]\phi[\to K^+K^-]$ data:

$$|\lambda_{\psi\phi}| = 0.964 \pm 0.019 \pm 0.007 . \qquad (4.13)$$

The deviation from unity at the $1.8\,\sigma$ level — which could well be an experimental fluctuation — would be surprisingly large in view of the discussion given above. In figure 11, we convert this result into a contour band in the $\theta_{\psi\phi}'$-$a_{\psi\phi}'$ plane. As expected, the central value would correspond to penguin effects too large to be consistent with the other constraints. Assuming the SM value of ϕ_s in eq. (1.2), we may also show the experimental result in eq. (4.8) as a band in this figure. This analysis illustrates the observation we made in the context with eqs. (3.9) and (3.10): in order to ensure a small phase shift of ϕ_s for large penguin parameters, strong phases around $\pm 90^\circ$ are needed. Interestingly, the data for $B_d^0 \to J/\psi\rho^0$ also suggest such a picture for the strong phases.

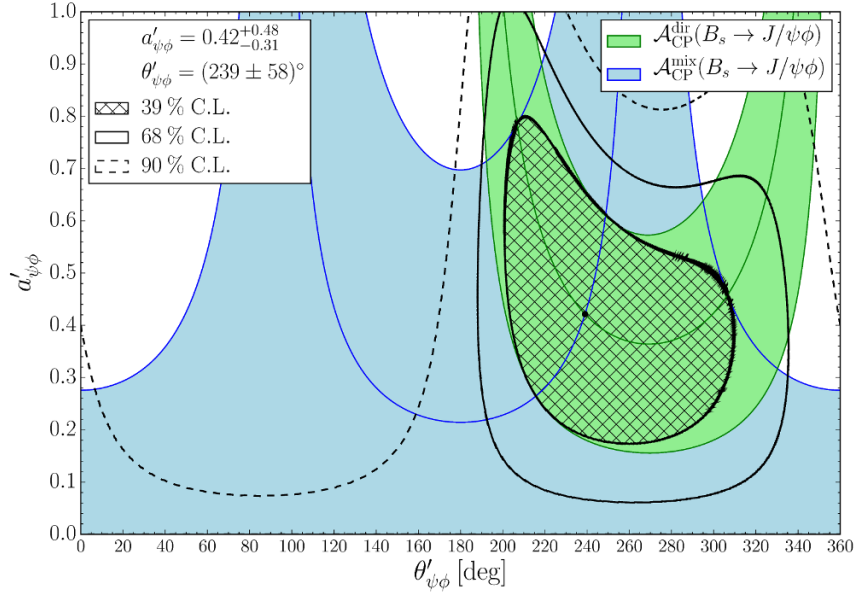**Figure 11**. Constraints in the $\theta'_{\psi\phi}$-$a'_{\psi\phi}$ plane following from the effective B_s^0-$\bar{B}_s^0$ mixing phase in eq. (4.8) and $|\lambda_{\psi\phi}|$ in eq. (4.13). Here we assume the SM value of ϕ_s in eq. (1.2).
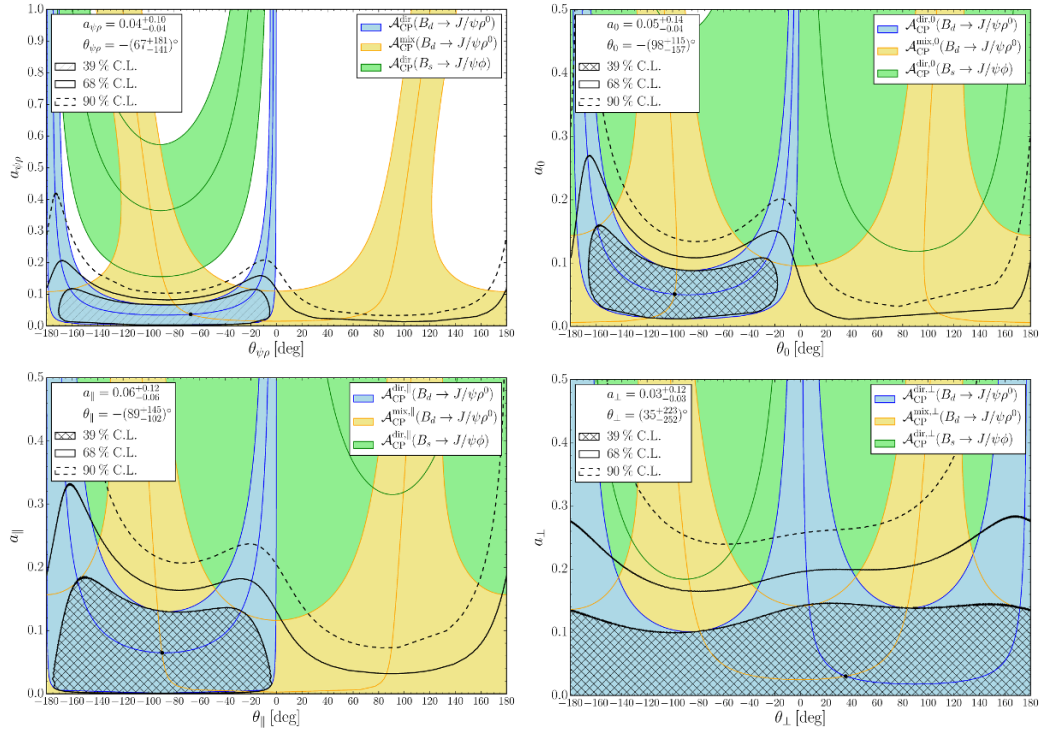

Figure 12. Determination of the penguin parameters a_f and θ_f from intersecting contours derived from the CP observables in $B_d^0 \to J/\psi\rho^0$. Superimposed are the confidence level contours obtained from a χ^2 fit to the data. The contour originating from the direct CP violation in $B_s^0 \to J/\psi\phi$ (see also figure 11) has been added for visual comparison, but is not taken into account in the fit.

4.3 The $B_d^0 \to J/\psi \rho^0$ channel

In analogy to $B_s^0 \to J/\psi K_S^0$ and $B_d^0 \to J/\psi \pi^0$, the decay $B_d^0 \to J/\psi \rho^0$ originates from $\bar{b} \to \bar{d} c \bar{c}$ quark-level transitions and has a decay amplitude of similar structure [10]:

$$\sqrt{2}\, A \left(B_d^0 \to (J/\psi \rho^0)_f \right) = -\lambda \mathcal{A}_f \left[1 - a_f e^{i\theta_f} e^{i\gamma} \right] , \tag{4.14}$$

where the factor of $\sqrt{2}$ is due to the wave function of the ρ^0. In analogy to $B_s^0 \to J/\psi \phi$, the $B_d^0 \to J/\psi \rho^0$ decay also shows mixing-induced CP violation, where an analysis of the $J/\psi \to \ell^+ \ell^-$ and $\rho^0 \to \pi^+ \pi^-$ decay products is required to disentangle the CP-even and CP-odd final states. In order to apply the formalism of section 2, we have to make the replacements

$$B_d^0 \to J/\psi \rho^0 : b_f e^{i\rho_f} \to a_f e^{i\theta_f}, \qquad \mathcal{N}_f \to -\frac{\lambda \mathcal{A}_f}{\sqrt{2}} . \tag{4.15}$$

In particular, we then obtain expressions for the "effective" mixing phases $\phi_{d,f}^{\mathrm{eff}} \equiv 2\beta_f^{\mathrm{eff}}$ by applying eq. (2.7). It should be emphasised that the corresponding penguin shifts are not doubly Cabibbo-suppressed. If we rescale the result in eq. (3.32) by $-1/\epsilon$, we expect hadronic penguin shifts of $\mathcal{O}(20°)$ in the $B_d^0 \to J/\psi \rho^0$ channel. However, as we noted after eqs. (3.9) and (3.10), and as we will see below, also the strong phases play an important role for the numerical values. The hadronic parameters in the $B_{s,d}^0 \to J/\psi K_S^0$ system and in $B_d^0 \to J/\psi \rho^0$ are generally expected to differ from one another.

The LHCb collaboration has recently reported the first experimental results for CP violation in the $B_d^0 \to J/\psi \rho^0$ channel [21]. The measurements of the polarisation-dependent effective B_d^0-$\bar{B}_d^0$ mixing phases are given as follows:

$$\phi_{d,0}^{\mathrm{eff}} = \left(44.1 \pm 10.2^{+3.0}_{-6.9} \right)^{\circ} , \tag{4.16}$$

$$\phi_{d,\parallel}^{\mathrm{eff}} - \phi_{d,0}^{\mathrm{eff}} = -\left(0.8 \pm 6.5^{+1.9}_{-1.3} \right)^{\circ} , \tag{4.17}$$

$$\phi_{d,\perp}^{\mathrm{eff}} - \phi_{d,0}^{\mathrm{eff}} = -\left(3.6 \pm 7.2^{+2.0}_{-1.4} \right)^{\circ} . \tag{4.18}$$

Within the uncertainties, no dependence on the final-state configuration f is detected. Assuming penguin parameters independent of f, i.e.

$$a_f \equiv a_{\psi\rho}, \qquad \theta_f \equiv \theta_{\psi\rho} \qquad \forall f \in \{0, \parallel, \perp\} \tag{4.19}$$

in analogy to the relations in eq. (4.4), the phase

$$\phi_d^{\mathrm{eff}} = \left(41.7 \pm 9.6^{+2.8}_{-6.3} \right)^{\circ} \tag{4.20}$$

and the CP asymmetries

$$\mathcal{A}_{\mathrm{CP}}^{\mathrm{dir}}(B_d \to J/\psi \rho) \equiv C_{J/\psi\rho} = -0.063 \pm 0.056^{+0.019}_{-0.014} \tag{4.21}$$

$$-\mathcal{A}_{\mathrm{CP}}^{\mathrm{mix}}(B_d \to J/\psi \rho) \equiv S_{J/\psi\rho} = -0.66^{+0.13}_{-0.12}{}^{+0.09}_{-0.03} \tag{4.22}$$

are extracted from the experimental analysis of the time-dependent angular distribution of the $B_d^0 \to J/\psi[\to \mu^+ \mu^-]\rho^0[\to \pi^+ \pi^-]$ decay products.

The formulae in section 2 allow the conversion of these results into the $B_d^0 \to J/\psi\rho^0$ penguin parameters. To this end, we assume again the CKMfitter value of γ in eq. (3.24). Moreover, we need the B_d^0-$\bar{B}_d^0$ mixing phase ϕ_d as an input for the analysis of the mixing-induced CP asymmetry. However, as we have actually extracted ϕ_d from the global fit discussed in section 3.4, we shall use the value in eq. (3.31) for the $B_d^0 \to J/\psi\rho^0$ analysis. In the LHCb study of ref. [21], corrections from penguin contributions to $B_d^0 \to J/\psi K_S^0$ were not taken into account.

The main results of the χ^2 fit to the data read as follows:

$$a_{\psi\rho} = 0.037^{+0.097}_{-0.037}\,, \qquad \theta_{\psi\rho} = -\left(67^{+181}_{-141}\right)^\circ\,, \qquad \Delta\phi_d^{\psi\rho} = -\left(1.5^{+12}_{-10}\right)^\circ\,. \qquad (4.23)$$

In figure 12, we show the corresponding confidence level contours with the bands of the individual observables. It is interesting to note that the current experimental measurement of $|\lambda_{\psi\phi}|$ from $B_s^0 \to J/\psi\phi$ is in slight tension with the results from $B_d^0 \to J/\psi\rho^0$. Should this turn out not to be a mere fluctuation of the data, which seems unlikely, the effect cannot be explained by penguin effects alone.

We have also explored a polarisation-dependent analysis of the penguin effects in $B_s^0 \to J/\psi\phi$ using the same strategy as for the above fit. The resulting confidence level contours are shown in figure 12. They are compatible with the polarisation-independent results in eq. (4.23), but the current uncertainties are too large to draw further conclusions. This analysis should be seen as an illustration and motivation for experimentalists to perform more precise polarisation-dependent measurements, which are the method of choice in the long run.

Neglecting exchange and penguin annihilation topologies (see figure 2), the SU(3) flavour symmetry allows us to convert the hadronic parameters of the $B_d^0 \to J/\psi\rho^0$ decay into their $B_s^0 \to J/\psi\phi$ counterparts [10]:

$$a_f' e^{i\theta_f'} = a_f e^{i\theta_f}\,, \qquad \mathcal{A}_f' = \mathcal{A}_f\,, \qquad (4.24)$$

allowing us to convert the penguin parameters in eq. (4.23) into the hadronic phase shift of the $B_s^0 \to J/\psi\phi$ decay. Parametrising possible SU(3)-breaking effects as in eq. (3.41) with $\xi = 1.00 \pm 0.20$ and $\delta = (0 \pm 20)^\circ$, we obtain

$$\Delta\phi_s^{\psi\phi} = \left[0.08^{+0.56}_{-0.72}\,(\text{stat})^{+0.15}_{-0.13}\,(\text{SU(3)})\right]^\circ\,, \qquad (4.25)$$

which is statistics limited, even when assuming larger SU(3)-breaking uncertainties. The power of mixing-induced CP violation in $B_d^0 \to J/\psi\rho^0$ for this determination is remarkable [21]. It should be compared with the current value of ϕ_s^{eff} in eq. (4.8), which is affected by significantly larger experimental uncertainties.

The contours in figure 12 do not rely on information from decay rates and are theoretically clean. As in the discussion of the $B_s^0 \to J/\psi K_S^0$ benchmark scenario in section 3.5, we may use the penguin parameters extracted from the CP asymmetries of $B_d^0 \to J/\psi\rho^0$ to determine the ratio of CP-conserving strong amplitudes, in analogy to eq. (3.44). The only conceptual difference is that polarisation-dependent studies should be performed in

the $B_d^0 \to J/\psi \rho^0$ and $B_s^0 \to J/\psi \phi$ systems. Following these lines, we obtain the amplitude ratios

$$\left| \frac{\mathcal{A}_0'(B_s \to J/\psi\phi)}{\mathcal{A}_0(B_d \to J/\psi\rho^0)} \right| = 1.06 \pm 0.07 \, (\text{stat}) \pm 0.04 \, (a_0, \theta_0) \tag{4.26}$$

$$\left| \frac{\mathcal{A}_\parallel'(B_s \to J/\psi\phi)}{\mathcal{A}_\parallel(B_d \to J/\psi\rho^0)} \right| = 1.08 \pm 0.08 \, (\text{stat}) \pm 0.05 \, (a_\parallel, \theta_\parallel) \tag{4.27}$$

$$\left| \frac{\mathcal{A}_\perp'(B_s \to J/\psi\phi)}{\mathcal{A}_\perp(B_d \to J/\psi\rho^0)} \right| = 1.24 \pm 0.15 \, (\text{stat}) \pm 0.06 \, (a_\perp, \theta_\perp) \,, \tag{4.28}$$

which are still consistent with the limit of no SU(3)-breaking corrections. These results can be compared with QCD calculations, such as the recent results obtained in ref. [17] within the perturbative QCD (PQCD) approach. Within naive factorisation, the LCSR form factors of ref. [48] (see table 8) yield

$$\left| \frac{\mathcal{A}_0'(B_s \to J/\psi\phi)}{\mathcal{A}_0(B_d \to J/\psi\rho^0)} \right|_{\text{fact}} = 1.43 \pm 0.42 \tag{4.29}$$

$$\left| \frac{\mathcal{A}_\parallel'(B_s \to J/\psi\phi)}{\mathcal{A}_\parallel(B_d \to J/\psi\rho^0)} \right|_{\text{fact}} = 1.37 \pm 0.20 \tag{4.30}$$

$$\left| \frac{\mathcal{A}_\perp'(B_s \to J/\psi\phi)}{\mathcal{A}_\perp(B_d \to J/\psi\rho^0)} \right|_{\text{fact}} = 1.25 \pm 0.15 \,. \tag{4.31}$$

Although the uncertainties are still very large, these numbers are consistent with the results in eqs. (4.26)–(4.28), and imply

$$\left| \frac{\mathcal{A}'}{\mathcal{A}} \right| = \left| \frac{\mathcal{A}_{\text{fact}}'}{\mathcal{A}_{\text{fact}}} \right| \left| \frac{1 + \mathcal{A}_{\text{non-fact}}'/\mathcal{A}_{\text{fact}}'}{1 + \mathcal{A}_{\text{non-fact}}/\mathcal{A}_{\text{fact}}} \right| \approx \left| \frac{\mathcal{A}_{\text{fact}}'}{\mathcal{A}_{\text{fact}}} \right| \,. \tag{4.32}$$

Consequently, either the non-factorisable contributions $\mathcal{A}_{\text{non-fact}}^{(\prime)}$ themselves or the difference (due to SU(3)-breaking effects) between the ratios $\mathcal{A}_{\text{non-fact}}'/\mathcal{A}_{\text{fact}}'$ and $\mathcal{A}_{\text{non-fact}}/\mathcal{A}_{\text{fact}}$ is small. In view of the discussion after eqs. (3.6) and (3.7), the latter option is favoured. A similar picture also arises for SU(3)-breaking effects in $B_d^0 \to \pi^+\pi^-$, $B_d^0 \to \pi^-K^+$, $B_s^0 \to K^+K^-$ decays, which exhibit a different decay dynamics [49]. In view of this observation, we get confidence in the first relation in eq. (4.24) (and the uncertainties assumed in eq. (3.41)). It is interesting to note that the experimental uncertainties of the ratios in eqs. (4.26)–(4.28) are already smaller or of similar size than the uncertainties of the theoretical calculations, which are challenging to improve.

4.4 The $B_s^0 \to J/\psi \overline{K}^{*0}$ channel

The decay $B_s^0 \to J/\psi \overline{K}^{*0}$ originates from $\bar{b} \to \bar{d}c\bar{c}$ quark-level processes and is the B_s^0-meson counterpart of the $B_d^0 \to J/\psi\rho^0$ mode. The CDF [24] and LHCb [42] collaborations have measured the $B_s^0 \to J/\psi \overline{K}^{*0}$ branching ratio. In the SM, the decay amplitude takes the form

$$A(B_d^0 \to (J/\psi \overline{K}^{*0})_f) = -\lambda \tilde{\mathcal{A}}_f \left[1 - \tilde{a}_f e^{i\tilde{\theta}_f} e^{i\gamma} \right] \,, \tag{4.33}$$

where we have introduced the tilde to distinguish the hadronic $B_s^0 \to J/\psi \bar{K}^{*0}$ parameters from their $B_d^0 \to J/\psi \rho^0$ counterparts. Using SU(3) flavour symmetry arguments and neglecting penguin annihilation and exchange topologies in $B_d^0 \to J/\psi \rho^0$, we obtain the relations

$$\tilde{a}_f e^{i\tilde{\theta}_f} = a_f e^{i\theta_f} \,, \qquad \tilde{\mathcal{A}}_f = \mathcal{A}_f \,. \tag{4.34}$$

In order to apply the formalism of section 2, we have to make the substitutions

$$B_s^0 \to J/\psi \bar{K}^{*0} : b_f e^{i\rho_f} \to \tilde{a}_f e^{i\tilde{\theta}_f} \,, \qquad \mathcal{N}_f \to -\lambda \tilde{\mathcal{A}}_f \,. \tag{4.35}$$

In contrast to the $B_d^0 \to J/\psi \rho^0$ channel, the $B_s^0 \to J/\psi \bar{K}^{*0}$ decay does *not* exhibit mixing-induced CP violation as the $J/\psi \bar{K}^{*0}$ final state is flavour specific, i.e. the pion and kaon charges of $\bar{K}^{*0} \to \pi^+ K^-$ and $K^{*0} \to \pi^- K^+$ distinguish between initially present B_s^0 and $\bar{B}_s^0$ mesons, respectively. Consequently, in order to determine the penguin parameters, we have to rely on direct CP violation and decay rate information [15]. For each of the final-state configurations $f \in \{0, \|, \perp\}$, we have a direct CP asymmetry $\mathcal{A}_{\mathrm{CP}}^{\mathrm{dir},f}$ and an observable corresponding to eq. (3.21):

$$\tilde{H}_f \equiv \frac{1}{\epsilon} \left| \frac{\mathcal{A}_f'}{\tilde{\mathcal{A}}_f} \right|^2 \frac{\mathrm{PhSp}\,(B_s \to J/\psi \phi)}{\mathrm{PhSp}(B_s \to J/\psi \bar{K}^{*0})} \frac{\mathcal{B}(B_s \to J/\psi \bar{K}^{*0})_{\mathrm{theo}}}{\mathcal{B}(B_s \to J/\psi \phi)_{\mathrm{theo}}} \frac{\tilde{f}_{\mathrm{VV},f}^{\mathrm{exp}}}{f_{\mathrm{VV},f}^{\mathrm{exp}}} \,, \tag{4.36}$$

where

$$f_{\mathrm{VV},f}^{\mathrm{exp}} \equiv \frac{\mathcal{B}(B_s \to (f)_f)_{\mathrm{exp}}}{\sum_f \mathcal{B}(B_s \to (f)_f)_{\mathrm{exp}}} \tag{4.37}$$

is the polarisation fraction of the $B_s \to f$ channel with $\sum_f f_{\mathrm{VV},f}^{\mathrm{exp}} = 1$. Also for the vector–vector modes the H_f observables use the "theoretical" branching ratio concept, which for B_s decays differs from the experimentally measured time-integrated branching ratio [29]. The conversion factors are similar to eq. (3.16) but become polarisation dependent. The measurement of these observables, which depend on $\tilde{a}_f$ and $\tilde{\theta}_f$ as well as γ, requires again an angular analysis of the decay products. Since γ is an input, we may determine the penguin parameters for the different final state configurations f [15].

In contrast to the analysis of $B_d^0 \to J/\psi \rho^0$, where mixing-induced CP violation plays the key role, this method is affected by hadronic uncertainties which enter through the $\tilde{H}_f$ ratios. The extraction of these quantities from the data involves ratios of strong amplitudes, which depend on hadronic form factors and non-factorisable effects. In ref. [17], a detailed analysis of these quantities has been performed within the PQCD approach. We shall return to this topic below.

Measurements of direct CP asymmetries of the $B_s^0 \to J/\psi \bar{K}^{*0}$ decay have not yet been performed. Using eq. (4.34), we expect them to equal those of $B_d^0 \to J/\psi \rho^0$:

$$\mathcal{A}_{\mathrm{CP}}^{\mathrm{dir}}(B_s \to J/\psi \bar{K}^{*0})_0 = -0.094 \pm 0.071 \,, \tag{4.38}$$

$$\mathcal{A}_{\mathrm{CP}}^{\mathrm{dir}}(B_s \to J/\psi \bar{K}^{*0})_\| = -0.12 \pm 0.12 \,, \tag{4.39}$$

$$\mathcal{A}_{\mathrm{CP}}^{\mathrm{dir}}(B_s \to J/\psi \bar{K}^{*0})_\perp = 0.03 \pm 0.22 \,, \tag{4.40}$$

where the CP asymmetries are defined as in ref. [15]. It will be interesting to confront these numbers with future experimental results.

5 Roadmap

In the era of the LHCb upgrade and Belle II, there will be a powerful interplay of the different decay channels discussed in this paper. The measurement of CP violation in the $B_s^0 \to J/\psi K_S^0$ decay will allow us to extract the corresponding penguin parameters in a theoretically clean way at LHCb and to control the penguin effects in the extraction of ϕ_d from $B_d^0 \to J/\psi K_S^0$ with the help of the U-spin symmetry [9, 32].

At Belle II, it will be important to measure CP violation in $B_d^0 \to J/\psi \pi^0$ and to resolve the current discrepancy between the BaBar and Belle measurements of the mixing-induced CP asymmetry (see eq. (3.26)). The penguin parameters can be determined in analogy to the $B_s^0 \to J/\psi K_S^0$ strategy [12, 13]. However, whereas the U-spin symmetry is sufficient in the case of the $B_{s,d}^0 \to J/\psi K_S^0$ system, the $B_d^0 \to J/\psi \pi^0$ mode is affected by further uncertainties due to penguin annihilation and exchange topologies, which arise in $B_d^0 \to J/\psi \pi^0$ but have no counterpart in $B_d^0 \to J/\psi K_S^0$. Some of these amplitudes are isospin suppressed (and thus expected to be very small) but not those competing with the penguin contributions. The annihilation and exchange topologies can be probed through $B_s^0 \to J/\psi \pi^0$ [14]. The LHCb collaboration does not see any evidence for the $B_s^0 \to J/\psi \rho^0$ channel in the current data [50].

Following these lines, the B_d^0-$\bar{B}_d^0$ mixing phase ϕ_d can be extracted with unprecedented precision. The key question is whether the comparison with the SM value $\phi_d^{\mathrm{SM}} = 2\beta$ will result in a discrepancy, thereby indicating a CP-violating NP phase ϕ_d^{NP}. Here the interplay between γ and the side R_b of the UT is crucial [51]:

$$\sin 2\beta = \frac{2R_b \sin\gamma(1 - R_b \cos\gamma)}{(R_b \sin\gamma)^2 + (1 - R_b \cos\gamma)^2} \, . \tag{5.1}$$

The precision will be governed by R_b [7, 33]. Future data collected at the Belle II experiment and theoretical progress will hopefully resolve the discrepancy between the determination of R_b from inclusive and exclusive semileptonic B decays [27]. The angle γ can be determined with high precision from $B \to D^{(*)}K^{(*)}$ decays, as given in eq. (3.37).

Measurements of the CP violation in $B_s^0 \to J/\psi \phi$ will play a key role for the determination of ϕ_s. It will be important to have polarisation-dependent analyses of $\phi_{s,f}^{\mathrm{eff}}$ available with a precision much higher than the pioneering LHCb results reported recently in ref. [20]. Different values would signal the presence of penguin effects and a violation of the relations for the penguin parameters in eq. (4.4). Measurements of the direct and mixing-induced CP-violating observables of the $B_d^0 \to J/\psi \rho^0$ channel allow us to determine the corresponding penguin parameters in a clean way [10]. Here the value of ϕ_d determined from the $B_{d,s}^0 \to J/\psi K_S^0$ system is needed as an input. Also in the $B_d^0 \to J/\psi \rho^0$ analysis it will be important to make final-state-dependent measurements. The experimental results of ref. [21] provide a fertile ground for these analyses. Using then the relations in eq. (4.24) allows us to determine the phase shifts $\Delta\phi_s^f$ and to extract the values of ϕ_s from the effective mixing phases $\phi_{s,f}^{\mathrm{eff}}$ of the $B_s^0 \to J/\psi \phi$ channel.

The penguin effects can also be probed by the $B_s^0 \to J/\psi \bar{K}^{*0}$ decay [15]. This channel provides direct CP asymmetries but no mixing-induced CP violation as the final state
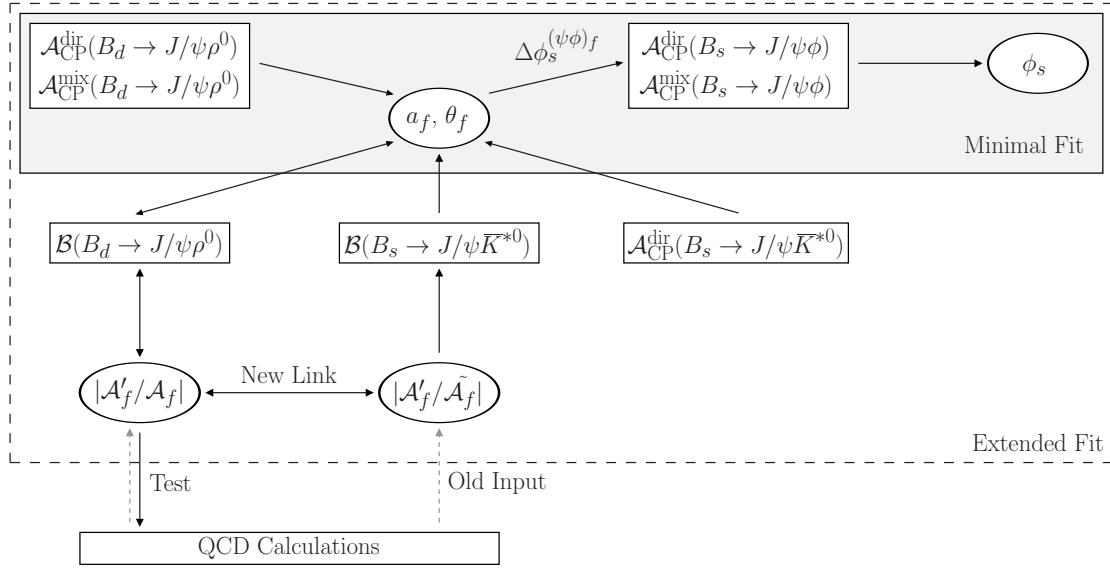
Figure 13. Flow chart of the combined analysis of the $B_d^0 \to J/\psi\rho^0$, $B_s^0 \to J/\psi\overline{K}^{*0}$ and $B_s^0 \to J/\psi\phi$ modes to simultaneously determine the penguin parameters, the ratio of SU(3)-breaking strong amplitudes, and the CP-violating B_s^0-$\bar{B}_s^0$ mixing phase ϕ_s.

is flavour-specific. In order to make use of the branching ratio information, ratios of strong amplitudes $|\mathcal{A}'_f/\tilde{\mathcal{A}}_f|$ are needed which introduce hadronic form-factor and non-factorisable uncertainties into the analysis. However, these ratios can actually be fixed through experiment. From the $B_d^0 \to J/\psi\rho^0$, $B_s^0 \to J/\psi\phi$ analysis, we may determine the ratios $|\mathcal{A}'_f/\mathcal{A}_f|$ in a theoretically clean way, as we discussed in eqs. (4.26)–(4.28) for the current data. Using the relation in eq. (4.34), we obtain

$$\left|\frac{\mathcal{A}'_f}{\mathcal{A}_f}\right| = \left|\frac{\mathcal{A}'_f}{\tilde{\mathcal{A}}_f}\right|, \tag{5.2}$$

which allows us to convert the $B_s^0 \to J/\psi\overline{K}^{*0}$ rate measurements into the $\tilde{H}_f$ observables. Finally, using also the relation

$$\tilde{a}_f e^{i\tilde{\theta}_f} = a_f e^{i\theta_f} = a'_f e^{i\theta'_f}, \tag{5.3}$$

it is possible to make a simultaneous χ^2 fit to the experimental data offered by the $B_s^0 \to J/\psi\phi$, $B_d^0 \to J/\psi\rho^0$, $B_s^0 \to J/\psi\overline{K}^{*0}$ system as illustrated in the flow chart in figure 13. This global analysis allows us to combine all the information offered by the penguin control channels in an optimal way and provides valuable insights into strong interactions as a by-product. Even though the direct CP asymmetry measurements in $B_s^0 \to J/\psi\overline{K}^{*0}$ are at present not yet available, we can already implement this strategy and extend the fits in figure 12 to include branching ratio information from $B_s^0 \to J/\psi\phi$, $B_d^0 \to J/\psi\rho^0$ and $B_s^0 \to J/\psi\overline{K}^{*0}$. The results of this analysis are

$$\left|\frac{\mathcal{A}'_0}{\mathcal{A}_0}\right| = 1.073^{+0.094}_{-0.073}, \qquad a_0 = 0.05^{+0.14}_{-0.04}, \qquad \theta_0 = -\left(98^{+115}_{-157}\right)^\circ, \tag{5.4}$$

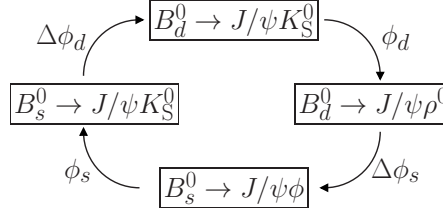**Figure 14**. Interplay between the decays used to measure the B_q^0-$\bar{B}_q^0$ mixing phases and the channels needed to control the penguin contributions in the former measurements.

$$\left|\frac{\mathcal{A}'_\parallel}{\mathcal{A}_\parallel}\right| = 1.088^{+0.114}_{-0.085}\,, \qquad a_\parallel = 0.06^{+0.12}_{-0.06}\,, \qquad \theta_\parallel = -\left(89^{+145}_{-102}\right)^\circ\,, \qquad (5.5)$$

$$\left|\frac{\mathcal{A}'_\perp}{\mathcal{A}_\perp}\right| = 1.21^{+0.18}_{-0.13}\,, \qquad a_\perp = 0.03^{+0.12}_{-0.03}\,, \qquad \theta_\perp = \left(35^{+223}_{-252}\right)^\circ\,. \qquad (5.6)$$

We observe that with the current experimental precision the additional branching ratio information does not have any impact on the determination of a_f and θ_f with respect to the fits to the $B_d^0 \to J/\psi\rho^0$ system only. The information is fully used to constrain the amplitude ratios $|\mathcal{A}'_f/\mathcal{A}_f|$, which were previously not included in the fit. To observe any impact on a_f and θ_f, the combined experimental precision on the H observables needs to be improved by at least an order of magnitude. Numerical differences in $|\mathcal{A}'_f/\mathcal{A}_f|$ compared to eqs. (4.26)–(4.28) arise due to the added information originating from the $B_s^0 \to J/\psi\bar{K}^{*0}$ system. This extended fit may be further refined by adding information from $B_s^0 \to J/\psi\rho^0$ to probe exchange and penguin annihilation topologies.

There is actually an interplay between the high-precision determinations of ϕ_d and ϕ_s. The point is that ϕ_d is needed as an input for the analysis of mixing-induced CP violation of $B_d^0 \to J/\psi\rho^0$ whereas ϕ_s is required for the analysis of mixing-induced CP violation of $B_s^0 \to J/\psi K_S^0$. We have illustrated these cross links in figure 14. Consequently, it will be advantageous to eventually perform a simultaneous analysis of the $B_{s,d}^0 \to J/\psi K_S^0$ and $B_s^0 \to J/\psi\phi$, $B_d^0 \to J/\psi\rho^0$, $B_s^0 \to J/\psi\bar{K}^{*0}$ systems.

For the search of NP in the era of the LHCb upgrade [40] and Belle II [4], it will be important to have determinations of both ϕ_d and ϕ_s available with the highest possible precision. We obtain an interesting correlation between these mixing phases if their NP phases in eq. (1.1) take the same value:

$$\phi_s^{\text{NP}} = \phi_d^{\text{NP}} \equiv \phi^{\text{NP}}. \qquad (5.7)$$

This relation, which was considered in refs. [52, 53] on a phenomenological basis, arises actually in extensions of the SM going beyond "minimal flavour violation" (MFV), which are characterised by flavour-universal CP-violating NP phases (for an overview, see ref. [54]). In this specific class of NP, referred to as non-$\overline{\text{MFV}}$ models, we obtain the following correlation:

$$\phi_s = \phi_d + \left(\phi_s^{\text{SM}} - \phi_d^{\text{SM}}\right), \qquad (5.8)$$

which allows an experimental test. In figure 15, we illustrate this relation both for the current situation and for the expected situation in the LHCb upgrade era. The future
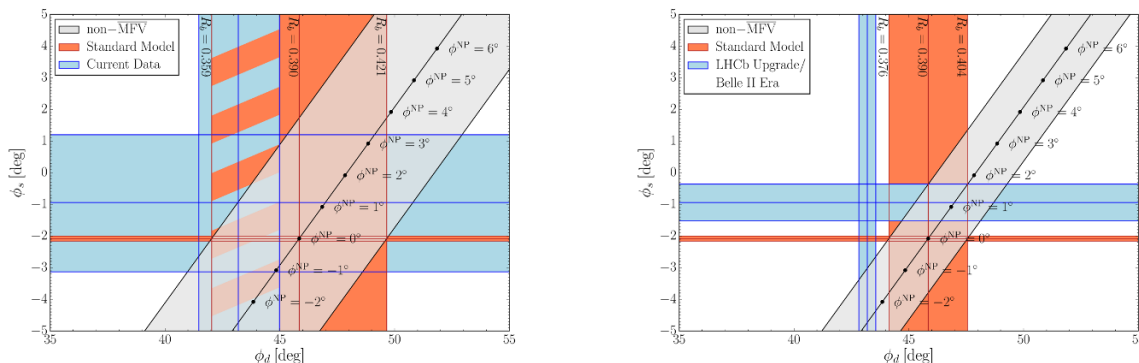
Figure 15. Illustration of the correlation between ϕ_s and ϕ_d for non-$\overline{\text{MFV}}$ models with flavour-universal CP-violating NP phases characterised by eq. (5.8): we show the current experimental situation (left) and extrapolate to the LHCb upgrade era (right).

uncertainty of the value of $\phi_d^{\text{SM}} = 2\beta$ will be fully governed by R_b (see eq. (5.1)), which enters also the band representing the relation in eq. (5.8). It will be interesting to confront these considerations with experimental data in the next decade.

6 Conclusions

The picture emerging from run I of the LHC suggests that we have to prepare ourselves to deal with smallish NP effects. For the determination of the B_q^0-$\bar{B}_q^0$ mixing phases ϕ_d and ϕ_s from CP violation measurements in $B_d^0 \to J/\psi K_S^0$ and $B_s^0 \to J/\psi \phi$, respectively, this implies that controlling higher order hadronic corrections, originating from doubly Cabibbo-suppressed penguin topologies, becomes mandatory. In this paper, we have outlined strategies to accomplish this task using the SU(3) flavour symmetry of QCD.

The penguin contributions to $B_d^0 \to J/\psi K_S^0$ can be controlled with the help of its U-spin partner $B_s^0 \to J/\psi K_S^0$. As the required CP violation measurements of the latter mode are not yet available, we have performed a global fit to current data for CP asymmetries and branching ratios of $B \to J/\psi(\pi/K)$ modes with similar dynamics to already constrain the hadronic penguin shift affecting the $B_d^0 \to J/\psi K_S^0$ channel. For the future LHCb upgrade era we have illustrated the potential of the $B_s^0 \to J/\psi K_S^0$ mode, which represents the cleanest penguin probe, with a benchmark scenario. In addition, we have discussed a strategy to probe non-factorisable U-spin-breaking effects in the $B_{s,d}^0 \to J/\psi K_S^0$ system.

The penguin contributions to $B_s^0 \to J/\psi \phi$ can be controlled with the help of the modes $B_d^0 \to J/\psi \rho^0$ and $B_s^0 \to J/\psi \bar{K}^{*0}$. We have analysed the first LHCb measurement of CP violation in $B_d^0 \to J/\psi \rho^0$, taking into account possible penguin effects in the required input for ϕ_d. In view of the excellent precision that can already be obtained in this analysis, the $B_d^0 \to J/\psi \rho^0$ mode is expected to play the key role for the control of the penguin effects in the determination of ϕ_s. We have proposed a new strategy to add the $B_s^0 \to J/\psi \bar{K}^{*0}$ data to this analysis in a global fit, which does not require knowledge of form factors for the interpretation of the decay rate information. It rather allows us to determine also hadronic parameters, which then provide insights into non-factorisable SU(3)-breaking effects. Adding

$B_s^0 \to J/\psi \rho^0$ to the analysis, also the impact of penguin annihilation and exchange topologies, which are expected to be small, can be probed through experimental data.

Finally, we propose a combined analysis of the $B_{s,d}^0 \to J/\psi K_S^0$ and $B_s^0 \to J/\psi \phi$, $B_d^0 \to J/\psi \rho^0$, $B_s^0 \to J/\psi \overline{K}^{*0}$ systems in order to simultaneously determine the mixing phases ϕ_d and ϕ_s, taking into account the cross-correlations between these modes in the control of the penguin effects. For the search of new sources of CP violation in the era of the LHCb upgrade and Belle II, simultaneous high-precision measurements of ϕ_d and ϕ_s are crucial ingredients. In extensions of the SM, such as non-$\overline{\text{MFV}}$ models, characteristic correlations between ϕ_d and ϕ_s arise which can then be tested. While the SM prediction of ϕ_s has already a precision much smaller than the LHCb upgrade sensitivity, the major limitation for ϕ_d^{SM} is given by the determination of $|V_{ub}/V_{cb}|$ entering the UT side R_b. Future progress on this long-standing challenge would be very desirable to complement the cutting-edge analyses of CP violation. We look forward to moving to the high-precision frontier!

Acknowledgments

A Contributions from annihilation topologies

The framework introduced in section 2 can be extended to allow for annihilation topologies A_c. The amplitude of the decay $B^+ \to J/\psi \pi^+$ can be written as

$$A(B^+ \to J/\psi \pi^+) = -\lambda \mathcal{A}_c \left[1 - a_c e^{i\theta_c} e^{i\gamma} \right], \tag{A.1}$$

where

$$\mathcal{A}_c \equiv \lambda^2 A \left[C_c + P_c^{(c)} - P_c^{(t)} \right] \tag{A.2}$$

is defined as in eq. (3.2), whereas

$$a_c e^{i\theta_c} = \tilde{a}_c e^{i\tilde{\theta}_c} + x e^{i\sigma} \tag{A.3}$$

with

$$\tilde{a}_c e^{i\tilde{\theta}_c} \equiv R_b \left[\frac{P_c^{(u)} - P_c^{(t)}}{C_c + P_c^{(c)} - P_c^{(t)}} \right] \tag{A.4}$$

and

$$x e^{i\sigma} \equiv R_b \left[\frac{A_c}{C_c + P_c^{(c)} - P_c^{(t)}} \right]. \tag{A.5}$$

The penguin parameter $\tilde{a}_c e^{i\tilde{\theta}_c}$ is defined in analogy to eq. (3.3), while the relative contribution from the annihilation topology is probed by $x e^{i\sigma}$. The direct CP asymmetry in $B^+ \to J/\psi \pi^+$ then takes the form

$$\mathcal{A}_{\text{CP}}^{\text{dir}} = \frac{2(\tilde{a}_c \sin \tilde{\theta}_c + x \sin \sigma) \sin \gamma}{1 - 2(\tilde{a}_c \cos \tilde{\theta}_c + x \cos \sigma) \cos \gamma + 2\tilde{a}_c x \cos(\tilde{\theta}_c - \sigma) + \tilde{a}_c^2 + x^2}, \tag{A.6}$$
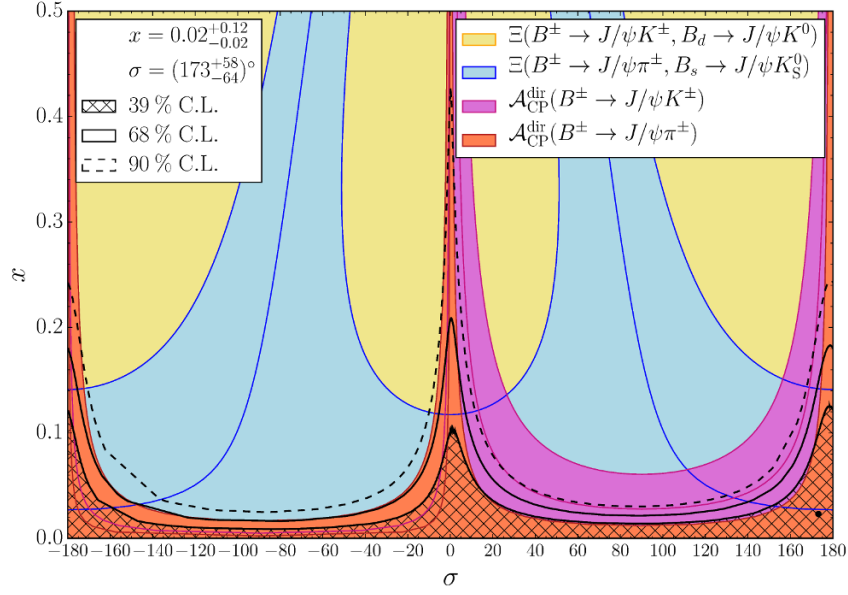
Figure 16. Determination of the parameters x and σ, which probe annihilation topologies in $B^+ \to J/\psi\pi^+$ and $B^+ \to J/\psi K^+$ decays, through intersecting contours corresponding to the current data for the CP asymmetries and branching ratio information. We show also the confidence level contours following from a χ^2 fit.

whereas the ratio $\Xi\left(B^\pm \to J/\psi\pi^\pm, B_s \to J/\psi K_S^0\right)$ depends on x and σ as

$$\Xi = \frac{1 - 2(\tilde{a}_c \cos\tilde{\theta}_c + x\cos\sigma)\cos\gamma + 2\tilde{a}_c x\cos(\tilde{\theta}_c - \sigma) + \tilde{a}_c^2 + x^2}{1 - 2\tilde{a}_c \cos\tilde{\theta}_c \cos\gamma + \tilde{a}_c^2} \,. \tag{A.7}$$

Similar expressions can be obtained for the direct CP asymmetry in $B^+ \to J/\psi K^+$ and the ratio $\Xi\left(B^\pm \to J/\psi K^\pm, B_d \to J/\psi K^0\right)$ by making the substitution

$$\tilde{a}_c \to \epsilon\tilde{a}_c' \,, \qquad \tilde{\theta}_c \to \tilde{\theta}_c' + \pi \,, \qquad x \to \epsilon x' \,, \qquad \sigma \to \sigma' + \pi \,. \tag{A.8}$$

Assuming

$$x' e^{i\sigma'} = x e^{i\sigma} \tag{A.9}$$

and universal penguin parameters, i.e.

$$\tilde{a}_c e^{i\tilde{\theta}_c} = \tilde{a}_c' e^{i\tilde{\theta}_c'} = a e^{i\theta}, \tag{A.10}$$

the annihilation parameters x and σ can be obtained from a χ^2 fit to the two direct CP asymmetries and the two Ξ ratios listed above. Including the observables γ (from eq. (3.24)), a and θ (from eq. (3.30)) as Gaussian constraints results in the solution

$$x = 0.02^{+0.12}_{-0.02} \,, \qquad \sigma = \left(173^{+58}_{-63}\right)^\circ \,, \tag{A.11}$$

with the corresponding confidence level contours shown in figure 16. The result is compatible with $x = 0$, which is consistent with our assumption to neglect contributions from annihilation topologies in the main χ^2 fit.

The results in eq. (A.11) assume external input for the penguin parameters a and θ, and therefore do not take into account the back reaction of a non-zero value of $xe^{i\sigma}$ on $ae^{i\theta}$. The annihilation topologies could lead to effects of similar size as the exchange and penguin annihilation topologies, which can be probed through the $B_s^0 \to J/\psi\pi^0$ decay. In the future, with stringent constraints on the branching ratio of this channel, an extended fit could be made, including all additional topologies. But then we expect to have also high-precision measurements of the CP violation in $B_s^0 \to J/\psi K_S^0$ available, allowing us to implement the strategy discussed in the main part of the paper. The extended fit would nevertheless offer an interesting cross-check to complement the picture of the penguin parameters.

References

[1] ATLAS collaboration, *Observation of a new particle in the search for the standard model Higgs boson with the ATLAS detector at the LHC*, *Phys. Lett.* **B 716** (2012) 1 [arXiv:1207.7214] [INSPIRE].

[2] CMS collaboration, *Observation of a new boson at a mass of* 125 *GeV with the CMS experiment at the LHC*, *Phys. Lett.* **B 716** (2012) 30 [arXiv:1207.7235] [INSPIRE].

[3] J. Ellis, *The beautiful physics of LHC run* 2, talk at *Beauty* 2014, Edinburgh U.K. July 14–18 2014 [arXiv:1412.2666] [INSPIRE].

[4] BELLE-II collaboration, T. Abe et al., *Belle II technical design report*, arXiv:1011.0352 [INSPIRE].

[5] N. Cabibbo, *Unitary symmetry and leptonic decays*, *Phys. Rev. Lett.* **10** (1963) 531 [INSPIRE].

[6] M. Kobayashi and T. Maskawa, *CP violation in the renormalizable theory of weak interaction*, *Prog. Theor. Phys.* **49** (1973) 652 [INSPIRE].

[7] J. Charles et al., *Predictions of selected flavour observables within the standard model*, *Phys. Rev.* **D 84** (2011) 033005 [arXiv:1106.4041] [INSPIRE]; for updates see *CKMfitter webpage*, http://ckmfitter.in2p3.fr/.

[8] L. Wolfenstein, *Parametrization of the Kobayashi-Maskawa matrix*, *Phys. Rev. Lett.* **51** (1983) 1945 [INSPIRE].

[9] R. Fleischer, *Extracting* γ *from* $B_{s(d)} \to J/\psi K_S$ *and* $B_{d(s)} \to D_{d(s)}^+ D_{d(s)}^-$, *Eur. Phys. J.* **C 10** (1999) 299 [hep-ph/9903455] [INSPIRE].

[10] R. Fleischer, *Extracting CKM phases from angular distributions of* $B_{d(s)}$ *decays into admixtures of CP eigenstates*, *Phys. Rev.* **D 60** (1999) 073008 [hep-ph/9903540] [INSPIRE].

[11] R. Fleischer, *Recent theoretical developments in CP-violation in the B system*, *Nucl. Instrum. Meth.* **A 446** (2000) 1 [hep-ph/9908340] [INSPIRE].

[12] M. Ciuchini, M. Pierini and L. Silvestrini, *The effect of penguins in the* $B_d \to J/\psi K^0$ *CP asymmetry*, *Phys. Rev. Lett.* **95** (2005) 221804 [hep-ph/0507290] [INSPIRE].

[13] M. Ciuchini, M. Pierini and L. Silvestrini, *Theoretical uncertainty in* $\sin 2\beta$: *an update*, arXiv:1102.0392 [INSPIRE].

[14] S. Faller, M. Jung, R. Fleischer and T. Mannel, *The golden modes $B^0 \to J/\psi K_{S,L}$ in the era of precision flavour physics*, *Phys. Rev.* **D 79** (2009) 014030 [arXiv:0809.0842] [INSPIRE].

[15] S. Faller, R. Fleischer and T. Mannel, *Precision physics with $B_s^0 \to J/\psi\phi$ at the LHC: the quest for new physics*, *Phys. Rev.* **D 79** (2009) 014005 [arXiv:0810.4248] [INSPIRE].

[16] M. Jung, *Determining weak phases from $B \to J/\psi P$ decays*, *Phys. Rev.* **D 86** (2012) 053008 [arXiv:1206.2050] [INSPIRE].

[17] X. Liu, W. Wang and Y. Xie, *Penguin pollution in $B \to J/\psi V$ decays and impact on the extraction of the B_s-$\bar{B}_s$ mixing phase*, *Phys. Rev.* **D 89** (2014) 094010 [arXiv:1309.0313] [INSPIRE].

[18] A.S. Dighe, I. Dunietz, H.J. Lipkin and J.L. Rosner, *Angular distributions and lifetime differences in $B_s \to J/\psi\phi$ decays*, *Phys. Lett.* **B 369** (1996) 144 [hep-ph/9511363] [INSPIRE].

[19] A.S. Dighe, I. Dunietz and R. Fleischer, *Extracting CKM phases and B_s-$\bar{B}_s$ mixing parameters from angular distributions of nonleptonic B decays*, *Eur. Phys. J.* **C 6** (1999) 647 [hep-ph/9804253] [INSPIRE].

[20] LHCb collaboration, *Precision measurement of CP violation in $B_s^0 \to J/\psi K^+ K^-$ decays*, *Phys. Rev. Lett.* **114** (2015) 041801 [arXiv:1411.3104] [INSPIRE].

[21] LHCb collaboration, *Measurement of the CP-violating phase β in $B^0 \to J/\psi\pi^+\pi^-$ decays and limits on penguin effects*, *Phys. Lett.* **B 742** (2015) 38 [arXiv:1411.1634] [INSPIRE].

[22] L. Zhang and S. Stone, *Time-dependent Dalitz-plot formalism for $B_q \to J/\psi h^+ h^-$*, *Phys. Lett.* **B 719** (2013) 383 [arXiv:1212.6434] [INSPIRE].

[23] R. Fleischer, *CP violation in the B system and relations to $K \to \pi\nu\bar{\nu}$ decays*, *Phys. Rept.* **370** (2002) 537 [hep-ph/0207108] [INSPIRE].

[24] CDF collaboration, T. Aaltonen et al., *Observation of $B_s^0 \to J/\psi K^*(892)^0$ and $B_s^0 \to J/\psi K_S^0$ decays*, *Phys. Rev.* **D 83** (2011) 052012 [arXiv:1102.1961] [INSPIRE].

[25] LHCb collaboration, *Measurement of the effective $B_s^0 \to J/\psi K_S^0$ lifetime*, *Nucl. Phys.* **B 873** (2013) 275 [arXiv:1304.4500] [INSPIRE].

[26] I. Dunietz, R. Fleischer and U. Nierste, *In pursuit of new physics with B_s decays*, *Phys. Rev.* **D 63** (2001) 114015 [hep-ph/0012219] [INSPIRE].

[27] PARTICLE DATA GROUP collaboration, K.A. Olive et al., *Review of particle physics*, *Chin. Phys.* **C 38** (2014) 090001 [INSPIRE].

[28] HEAVY FLAVOR AVERAGING GROUP collaboration, Y. Amhis et al., *Averages of b-hadron, c-hadron and τ-lepton properties as of early* 2012, arXiv:1207.1158 [INSPIRE]; for updates see *Heavy Flavor Averaging Group webpage*, http://www.slac.stanford.edu/xorg/hfag/.

[29] K. De Bruyn et al., *Branching ratio measurements of B_s decays*, *Phys. Rev.* **D 86** (2012) 014027 [arXiv:1204.1735] [INSPIRE].

[30] R. Fleischer and T. Mannel, *Constraining the CKM angle γ and penguin contributions through combined $B \to \pi K$ branching ratios*, *Phys. Rev.* **D 57** (1998) 2752 [hep-ph/9704423] [INSPIRE].

[31] R. Fleischer and S. Recksiegel, *General lower bounds for $b \to d$ penguin processes*, *Phys. Rev.* **D 71** (2005) 051501 [hep-ph/0409137] [INSPIRE].

[32] K. De Bruyn, R. Fleischer and P. Koppenburg, *Extracting γ and penguin topologies through CP-violation in $B_s^0 \to J/psi K_S$*, *Eur. Phys. J.* **C 70** (2010) 1025 [`arXiv:1010.0089`] [INSPIRE].

[33] A. Bevan et al., *Standard model updates and new physics analysis with the unitarity triangle fit*, `arXiv:1411.7233` [INSPIRE]; for updates see *UTfit collaboration webpage*, http://www.utfit.org/.

[34] BELLE collaboration, S.E. Lee et al., *Improved measurement of time-dependent CP-violation in $B^0 \to J/\psi \pi^0$ decays*, *Phys. Rev.* **D 77** (2008) 071101 [`arXiv:0708.0304`] [INSPIRE].

[35] BABAR collaboration, B. Aubert et al., *Evidence for CP-violation in $B^0 \to J/\psi \pi^0$ decays*, *Phys. Rev. Lett.* **101** (2008) 021801 [`arXiv:0804.0896`] [INSPIRE].

[36] A. Bharucha, *Two-loop corrections to the $B \to \pi$ form factor from QCD sum rules on the light-cone and $|V_{ub}|$*, *JHEP* **05** (2012) 092 [`arXiv:1203.1359`] [INSPIRE].

[37] A. Khodjamirian, T. Mannel, A.A. Pivovarov and Y.-M. Wang, *Charm-loop effect in $B \to K^{(*)} \ell^+ \ell^-$ and $B \to K^* \gamma$*, *JHEP* **09** (2010) 089 [`arXiv:1006.4945`] [INSPIRE].

[38] G. Duplancic and B. Melic, *$B, B_s \to K$ form factors: an update of light-cone sum rule results*, *Phys. Rev.* **D 78** (2008) 054015 [`arXiv:0805.4170`] [INSPIRE].

[39] P. Ball, *$|V_{ub}|$ from UTangles and $B \to \pi \ell \nu$*, *Phys. Lett.* **B 644** (2007) 38 [`hep-ph/0611108`] [INSPIRE].

[40] LHCb collaboration, *Implications of LHCb measurements and future prospects*, *Eur. Phys. J.* **C 73** (2013) 2373 [`arXiv:1208.3355`] [INSPIRE].

[41] LHCb collaboration, *Measurement of CP asymmetry in $B_s^0 \to D_s^\mp K^\pm$ decays*, *JHEP* **11** (2014) 060 [`arXiv:1407.6127`] [INSPIRE].

[42] LHCb collaboration, *Measurement of the $B_s^0 \to J/\psi \bar{K}^{*0}$ branching fraction and angular amplitudes*, *Phys. Rev.* **D 86** (2012) 071102 [`arXiv:1208.0738`] [INSPIRE].

[43] LHCb collaboration, *Measurement of the fragmentation fraction ratio f_s/f_d and its dependence on B meson kinematics*, *JHEP* **04** (2013) 001 [`arXiv:1301.5286`] [INSPIRE].

[44] LHCb collaboration, *Updated average f_s/f_d b-hadron production fraction ratio for 7 TeV pp collisions*, LHCb-CONF-2013-011, CERN, Geneva Switzerland (2013).

[45] R. Fleischer, N. Serra and N. Tuning, *A new strategy for B_s branching ratio measurements and the search for new physics in $B_s^0 \to m u^+ m u^-$*, *Phys. Rev.* **D 82** (2010) 034038 [`arXiv:1004.3982`] [INSPIRE].

[46] J.L. Rosner, *Determination of pseudoscalar charmed meson decay constants from B meson decays*, *Phys. Rev.* **D 42** (1990) 3732 [INSPIRE].

[47] A. Lenz, *B-mixing in and beyond the standard model*, talk at *CKM* 2014, Vienna Austria September 8–12 2014 [`arXiv:1409.6963`] [INSPIRE].

[48] P. Ball and R. Zwicky, *$B_{d,s} \to \rho, \omega, K^*, \phi$ decay form-factors from light-cone sum rules revisited*, *Phys. Rev.* **D 71** (2005) 014029 [`hep-ph/0412079`] [INSPIRE].

[49] R. Fleischer and R. Knegjens, *In pursuit of new physics with $B_s^0 \to K^+ K^-$*, *Eur. Phys. J.* **C 71** (2011) 1532 [`arXiv:1011.1096`] [INSPIRE].

[50] LHCb collaboration, *Measurement of resonant and CP components in $\bar{B}_s^0 \to J/\psi \pi^+ \pi^-$ decays*, *Phys. Rev.* **D 89** (2014) 092006 [`arXiv:1402.6248`] [INSPIRE].

[51] A.J. Buras and R. Fleischer, *Quark mixing, CP-violation and rare decays after the top quark discovery*, *Adv. Ser. Direct. High Energy Phys.* **15** (1998) 65 [hep-ph/9704376] [INSPIRE].

[52] P. Ball and R. Fleischer, *Probing new physics through B mixing: status, benchmarks and prospects*, *Eur. Phys. J.* **C 48** (2006) 413 [hep-ph/0604249] [INSPIRE].

[53] A.J. Buras and D. Guadagnoli, *Correlations among new CP-violating effects in $\Delta F = 2$ observables*, *Phys. Rev.* **D 78** (2008) 033005 [arXiv:0805.3887] [INSPIRE].

[54] A.J. Buras and J. Girrbach, *Towards the identification of new physics through quark flavour violating processes*, *Rept. Prog. Phys.* **77** (2014) 086201 [arXiv:1306.3775] [INSPIRE].